



Characterization of land degradation along the receding Dead Sea coastal zone using airborne laser scanning

Sagi Filin^{a,*}, Yoav Avni^b, Amit Baruch^a, Smadar Morik^a, Reuma Arav^a, Shmuel Marco^c

^a Mapping and Geo-Information Engineering, Technion - Israel Institute of Technology, Haifa, 32000, Israel

^b Geological Survey of Israel, Jerusalem, 95501, Israel

^c Department of Geophysics and Planetary Sciences, Tel-Aviv University, Tel-Aviv, 69978, Israel

ARTICLE INFO

Article history:

Received 27 December 2011

Received in revised form 25 September 2013

Accepted 15 October 2013

Available online 24 October 2013

Keywords:

Soil erosion
Coastal processes
Gully incision
Sinkholes
Laser scanning
Dead Sea

ABSTRACT

The Dead Sea, the lowest place on the Earth's continents, was at its highest level in 1896, reaching an elevation of ~388.4 m below mean sea level (m.b.m.s.l) and ~390 m in the early 1920s. Since then it has almost constantly been dropping, reaching the level of 426 m.b.m.s.l in 2013. Since the late 1990s its level has been decreasing by approximately 1 my^{-1} . The rapid lake retreat accelerates large-scale environmental deterioration, including soil erosion, land degradation, rapid headcut migration and widespread development of collapse sinkhole fields. These geomorphic elements threaten the natural environment and anthropogenic infrastructure.

We provide an overview of the geomorphic processes in the form of soil erosion, channel incision, land degradation, and the development of collapse sinkholes. We take advantage of the high-resolution airborne laser scanning technology for three-dimensional detection of surficial changes, quantification of their volumes, and documentation of the present state of the terrain with utmost accuracy and precision. This type of information and the identification of future trends are vital for proper planning of any rapidly-changing environment.

© 2013 Elsevier B.V. All rights reserved.

1. Introduction

Environmental deterioration in arid and semi-arid regions is a cause for increased concern in the international community (e.g., Mainguet, 1991; UNCCD, 1995; Bruins and Lithwick, 1998; UNYDD, 2006). This concern is driven by the urgent global need to protect the environment, in particular the soil cover, biomass, agricultural crops, and infrastructure; all are critical for maintaining the natural biodiversity and modern infrastructure.

Among the indicators for environmental deterioration in the semi-arid regions is the shrinkage of water bodies (e.g., Lake Chad, the Aral Sea, and the Dead Sea) mainly a consequence of increased usage of fresh water for irrigation and domestic needs (Yechieli et al., 1993; Glazovsky, 1995; Mainguet and Le'tolle, 1998). Due to the water-level drop, the newly exposed areas are subjected to erosion processes such as development of gullies and headcuts within unconsolidated coastal material (Campbell, 1989; Summerfield, 1991; Mainguet and Le'tolle, 1998; Avni et al., 2005). Channeling of fresh-water springs into newly developed deep gullies often causes destruction of wetland environments that previously existed along the lakes' coastal zone. These geomorphic changes may lead to total destruction of past environments and to the drying-up of the former fresh water wetlands that are subjected to de-watering, high evaporation and replacement by salty soils (Mainguet and Le'tolle, 1998; Avni et al., 2005; Bowman et al., 2007).

The Dead Sea level drop has reached rates of 1 my^{-1} in the last decades and even higher in recent years (Fig. 1c). This higher rate is a result of the combined effects of human interference and long-term, small scale, climate-induced change of the water balance in the entire 42,000 km² drainage basin. This process has led to a large-scale shrinkage of the lake and to incision of numerous new gullies, which are gradually migrating upstream within the newly exposed coastal zone. Additionally, thousands of collapse sinkholes have developed since the 1980s within the newly exposed areas of the declining Dead Sea. Both sinkhole development and gully incision have caused heavy damage to the existing infrastructure and halted modern development along considerable parts of the Dead Sea shores (Avni et al., 2005; Abelson et al., 2006). As these ongoing processes threaten to inflict even greater damage in the future, it is important to characterize them and detect incipient destructive processes as early as possible.

To this end we analyze the results from an airborne laser scanning survey of the current geomorphic system configuration of the western coastal plain of the Dead Sea. Previously, these three dimensional processes have been monitored using either classical geodetic techniques or simple 2D interpretation of aerial analog images. This paper analyzes processes along the Dead Sea shores as an example for land degradation influenced by lowering lake levels. Because Dead Sea water levels have been well-documented since the 1920s and tectonic motions have been negligible during this relatively short period (Garfunkel et al., 1981), we can convert spatial data into time, e.g., the age of each fossil shoreline in this sequence as well as any exposed surface previously covered by the lake can be straightforwardly determined. The choice of airborne laser

* Corresponding author. Tel.: +972 4 829 5855; fax: +972 4 829 5708.
E-mail address: filin@technion.ac.il (S. Filin).

scanning is motivated by the dense 3D description, the high accuracy of the data, and the level of detail that the system provides. The 3D information (point cloud) facilitates a high level of cost-effective automation in detection and analysis of geomorphic phenomena. These characteristics are of great value for detailed analysis of wide regions, for examining the evolution of existing phenomena, and particularly for detecting the appearance of new features, some of which are small, but significant in their lateral/cumulative effect.

2. Study area

The Dead Sea Basin (Fig. 1a,b), the lowest place on Earth's continents, is surrounded by active, fault-controlled escarpments, 600–1100 m high. The western escarpments are composed of Cretaceous limestone, dolomite and marl strata, whereas the eastern escarpment exposes older strata of late Precambrian to Cretaceous composed of volcanoclastic rocks, sandstone, limestone and dolomite (Sneh et al., 1998). During the Quaternary the Dead Sea Basin hosted a series of hypersaline lakes, the last of which is the Dead Sea. During glacial periods these lakes reached levels significantly higher than today. For example, the highest stand of Lake Lisan of the last glacial period was about 160 m below mean sea level (m.b.m.s.l). It was followed by a rapid drop and stabilized in the Holocene around 400 m.b.m.s.l with fluctuations of a few tens of meters (Klein and Flohn, 1987). The Dead Sea level in 1896 was ~388.4 m.b.m.s.l and ~390 m in the early 1920s. Since the 1930s, the construction of a dam at the outlet of the Sea of Galilee and an increased diversion of Jordan River water, the main source of water to the Dead Sea, caused a continuous level drop that accelerated since the 1970s. When levels dropped to 399.6 m.b.m.s.l in 1977, the southern shallow basin dried and the potash pans that were constructed there received the brine through channels from the northern basin. In 2013 the level of the lake was 426 m.b.m.s.l.

2.1. Modification of the geomorphic system

The geomorphic units associated with the rapid lake-level drop and the consequent instability of the geomorphic system consist of: i) *coastal flats* – a rapid widening of the western coastal plain, up to 3 km since 1930 till its present location, exposing two major substrates: coarse gravels deposited in proximal areas of alluvial fans and fine-grained mud composed of mainly silt and clay, which were deposited in the distal parts of the alluvial fans. As the lake retreats and the coastal zone widens, the mudflats become more dominant (Fig. 2a); ii) *newly exposed steep slopes* – attributed to either slopes developed along the distal edge of coarse alluvial fans, or to exposure of active-fault controlled slopes (Fig. 2b); iii) *deserted beach ridges* – related to wave action during spring storms. The position of each ridge marks the uppermost elevation that the lake level has reached during the end of the wet season, before the gradual retreat during the long, dry one (Fig. 2a,b); iv) *sinkholes* – observed in both the mudflats and alluvial fans. Deeper ones are found in the alluvial fans while shallower and wider ones in the mudflats (Abelson et al., 2006; Filin et al., 2011). In most cases the sinkhole formation is attributed to subsurface caverns that evolve by dissolution of a ~20–50 m deep salt layer because of the replacement of the hyper saline groundwater with present fresh water, as the local water table follows the drop of the lake level (Abelson et al., 2006; Yechieli et al., 2006; Filin et al., 2011). In some cases, sinkholes appear in swarms and large fields, up to 100 per site (Fig. 2c); v) *gullies* – which develop due to rapid incision within the exposed mud flats (Fig. 2d), commonly keep in pace by deepening and elongation in opposite directions: downstream toward the dropping lake and upstream toward the alluvial fans due to headcut migration and incision (Fig. 2e); and vi) *stream channels* – which developed at

the outlet of major drainage basins within the gravelly fans and migrate downstream. Incision of both gullies and stream channels is accelerated during flash floods, which characterize the flow regime in the desert environment surrounding the Dead Sea. The rapid incision is endangering the modern infrastructure along the coast (Fig. 2f).

2.2. Sites analyzed in this study

Three localities have been selected for scanning, representing and illustrating various aspects of the Dead Sea's dynamic environment. Their description is from south to north (Fig. 1b).

Ze'elim fan (lat. 31°22', long. 35°24') – Located at the outlet of the Ze'elim ~250 km² drainage basin and spans an area of about 10 km². It was initiated during the late Pleistocene–Holocene transition, following the retreat of the Late Pleistocene Lake Lisan (Begin et al., 1974; Ken-Tor et al., 2001).

Hever fan (lat. 31°20', long. 35°25') – A major fan in the region, located at the outlet of the Hever 175-km² drainage basin and spans an area larger than 5 km². The fan is composed of coarse gravels and its outlet towards the receding lake features a pattern of delicate braided channels. Because of the coarse material, the channels here are wider and shallower than the gullies developed in the distal mudflat exposed in Ze'elim.

Hazon fan and Mineral Beach (lat. 31°32', long. 35°23') – A resort in the central part of the Dead Sea, near the Hazon outlet. The Hazon creek, which drains an area of 41 km², forms a 0.7 km² fan composed of coarse Holocene fluvial pebbles. The Holocene fan is now incised by stream channels as a result of the lake retreat, similar to other Dead Sea fans. A wide mudflat on the southern side of the fan is dotted with an elongated cluster of sinkholes, striking north-northwest.

3. Methods

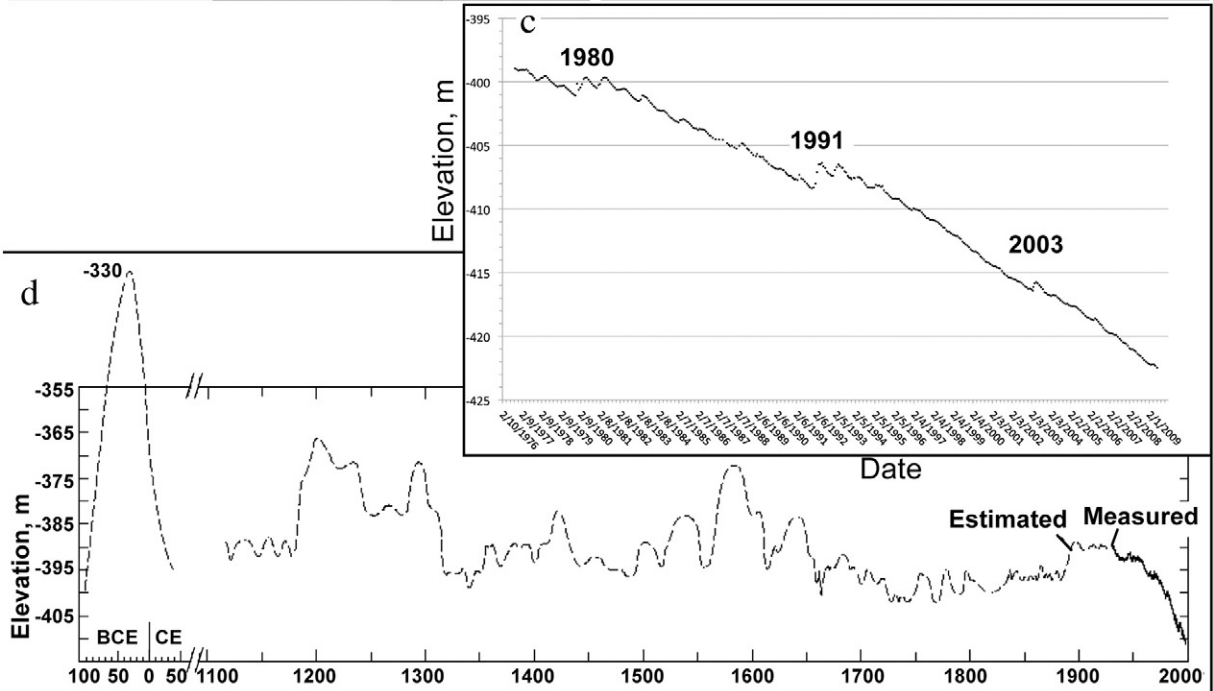
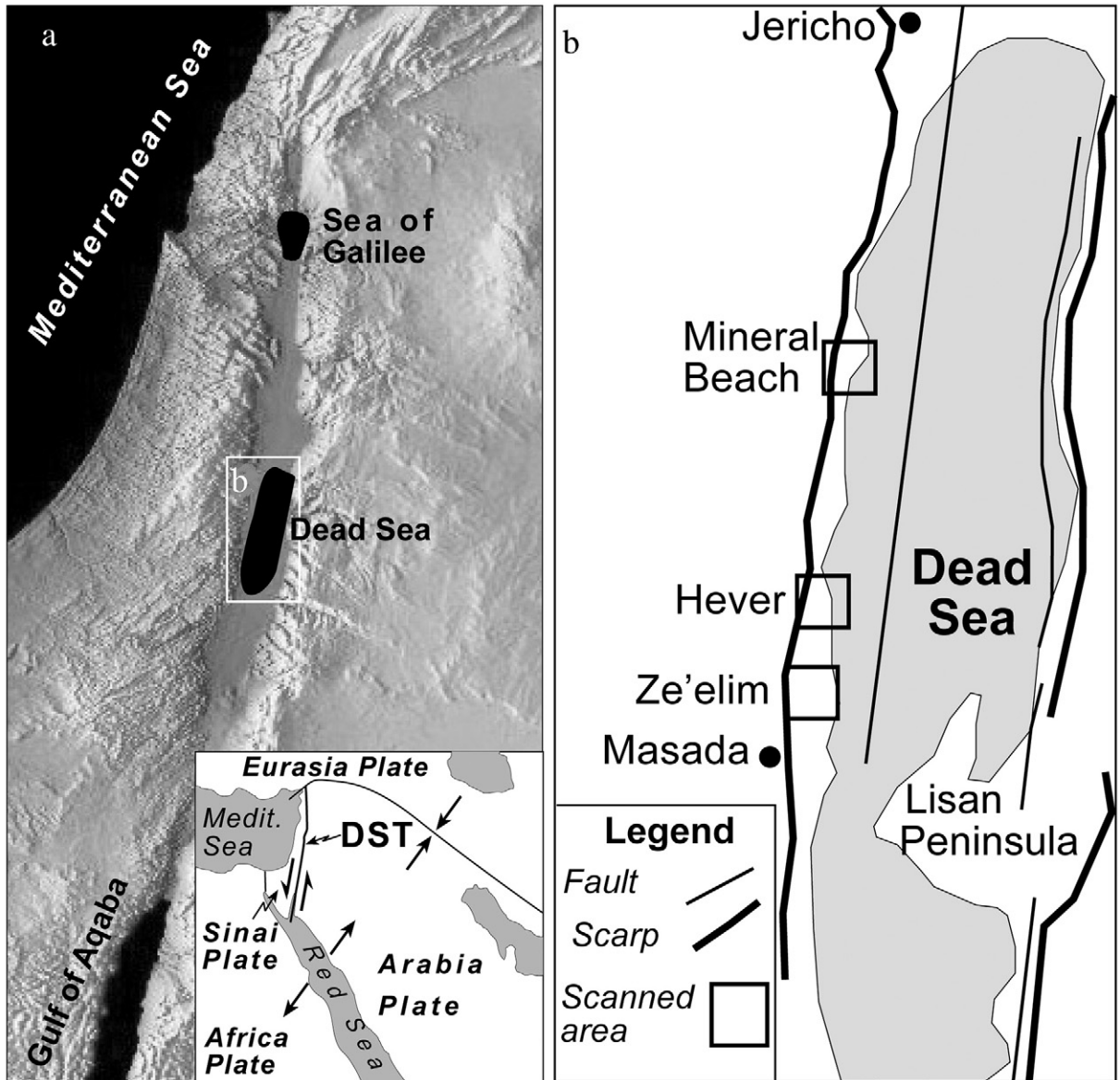
High-resolution airborne laser data for the three study sites about 30 km² in area were acquired using the Optech 2050 scanner, operating at 50 KHz. The flying altitude was ~500 m above ground level (m.a.g.l), leading to a sampling density of about 4 ptsm⁻². Determination of this point density was guided by the fine nature of some of the geomorphic features, e.g., small channels and embryonic sinkholes.

Validation of the laser scanning data accuracy was carried out via a GPS field survey. The new Israeli GPS virtual real-time network was used for this test as a reference station (enabling a measurement accuracy of about 2 cm horizontal and about 5 cm vertical). Comparison of the GPS survey (total of 200 measurements) to the laser scanning data shows a standard deviation of ± 10 cm with only eight points (4%) offset more than 25 cm.

As laser ranges are measured to objects illuminated by the laser beam, some returns arrive from the bare earth, while others from off-terrain objects. To analyze the region's morphology, off-terrain objects have been removed from the data. We applied a model proposed by Akel et al. (2007), which uses global orthogonal functions for a coarse separation of terrain and detached objects returns, and then introduces a surface refinement phase that adds fine terrain details that were skipped in the global phase. The global functions are given as a set of orthogonal polynomials whose coefficients are estimated robustly. Weights of points with a positive residual are reduced between iterations, thereby strengthening the influence of terrain points. The refinement phase adds points that conform to the general terrain shape via a local surface continuity test.

The relevant geomorphic features are characterized by a drop in the surface topography, forming a relatively sharp transition between the ground and object. Although a functional description which is driven by a gradient strength analysis ($|\nabla_x^2 + \nabla_y^2|$) may be appropriate, the rough

Fig. 1. The Dead Sea region and lake level variations. a) Location of the Dead Sea. b) Location of three observation areas. c.) Lake level record since 1976. Episodes of level rise superposed on the general lowering appeared in 1981, 1992, and 2003. d) Lake level of the last two millennia (after Klein and Flohn, 1987).



surface texture that characterizes alluvial fans generates rather noisy responses, which are hard to discriminate using an edge driven analysis (Fig. 3). We identify surface features via the analysis of principal curvature values, seeking the actual entities rather than their borders. The two principal curvatures (the minimal and positive values) of a given point can be estimated by the eigenvalues of the Hessian form, \mathbf{H}

$$\mathbf{H} = \begin{pmatrix} \frac{\partial^2 Z}{\partial x^2} & \frac{\partial^2 Z}{\partial x \partial y} \\ \frac{\partial^2 Z}{\partial x \partial y} & \frac{\partial^2 Z}{\partial y^2} \end{pmatrix} \quad (1)$$

where Z is the surface elevation derived from the airborne laser scanning data. The partial second-order derivatives are computed numerically via

$$\begin{aligned} \frac{\partial^2 Z}{\partial x^2} &= (Z_{y_0, x_0+d} - 2 \cdot Z_{y_0, x_0} + Z_{y_0, x_0-d}) / d^2 \\ \frac{\partial^2 Z}{\partial y^2} &= (Z_{y_0+d, x_0} - 2 \cdot Z_{y_0, x_0} + Z_{y_0-d, x_0}) / d^2 \\ \frac{\partial^2 Z}{\partial xy} &= (-Z_{y_0-d, x_0-d} + Z_{y_0-d, x_0+d} + Z_{y_0+d, x_0-d} - Z_{y_0+d, x_0+d}) / 4d^2 \end{aligned} \quad (2)$$

with d being the window size. The actual eigenvalues, λ_{\max} and λ_{\min} , are then computed via

$$\lambda_{\max, \min} = \frac{(\frac{\partial^2 Z}{\partial x^2} + \frac{\partial^2 Z}{\partial y^2}) \pm \sqrt{(\frac{\partial^2 Z}{\partial x^2} - \frac{\partial^2 Z}{\partial y^2})^2 + 4(\frac{\partial^2 Z}{\partial xy})^2}}{2} \quad (3)$$

This numerical estimation scheme easily adapts to the variety of sizes, shapes, and forms that the geomorphic features have.

The geomorphic feature characteristics are defined by the eigenvalues, particularly by their sign, which associates a point with a specific feature. For example, gully-related responses will be theoretically characterized by $\lambda_{\max} > 0$ and $\lambda_{\min} = 0$. Common detection practices apply a fixed kernel size and search for sufficiently strong responses, where thresholds are set empirically through trial and error. In practice, it is almost impossible to set a predefined threshold value that captures “strong” responses for all the diverse object appearances while suppressing surface texture effects. Here, the eigenvalue computation is performed in a multi-scale manner, from fine to coarse, searching for “significant” responses. Considering the eigenvalues’ magnitude, which

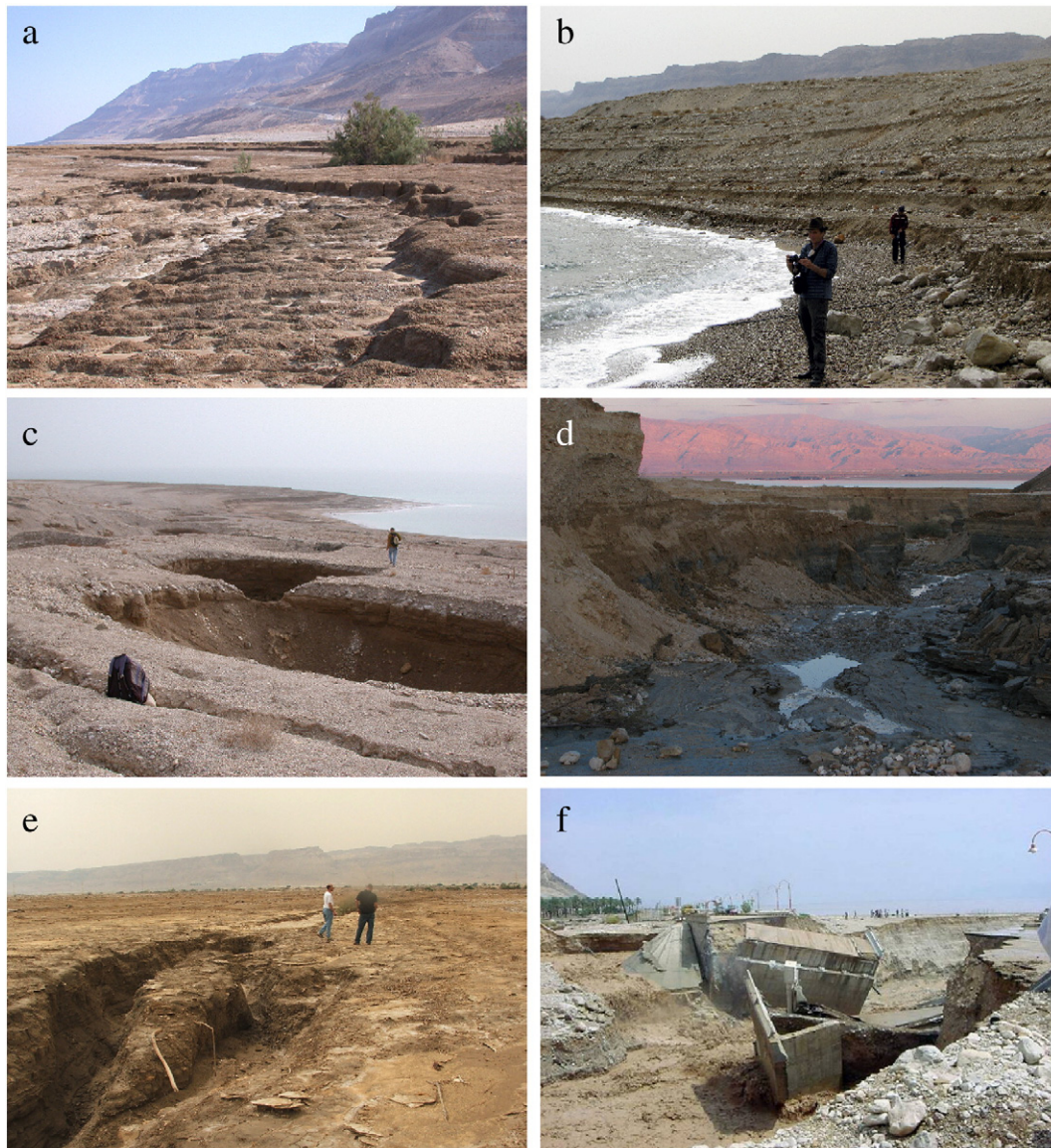


Fig. 2. Geomorphic features along the Dead Sea coastal plains. a) Newly exposed slopes with conspicuous shorelines. b) Deserted beachridge. c) Sinkholes. d) Gully incision. e) Upstream gully headcut. f) Modern infrastructure damaged by a flashflood on the Dead Sea coast.

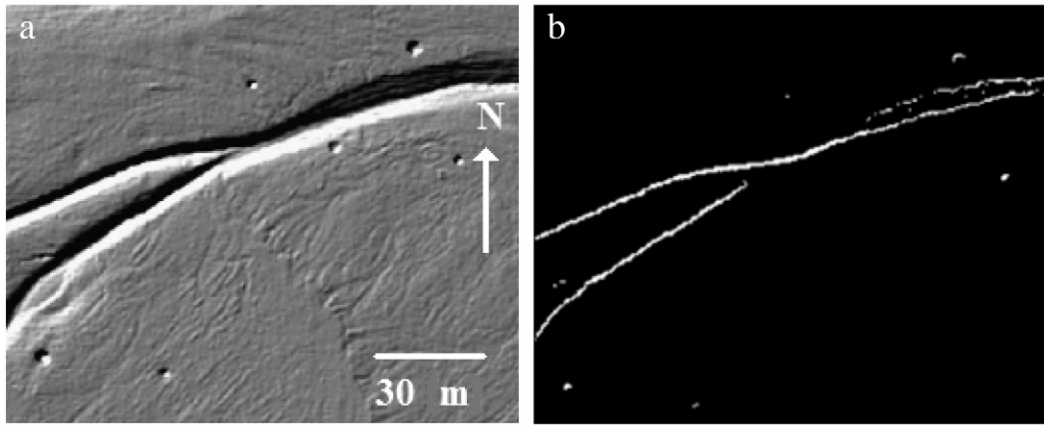


Fig. 3. First-order derivative based geomorphic feature analysis. a) A section in which two gullies converge into one. b) First order derivatives of this part showing partial extraction because of the difficulty in setting object-to-background transition thresholds.

defines the dominance of the phenomena, it is important to set upper and lower bound response levels, e.g., $|\lambda_{\min}| > \varepsilon_1$ or $|\lambda_{\min}| < \varepsilon_2$, with ε_1 and ε_2 as threshold values. We define them theoretically by deriving accuracy estimates for λ as a function of the laser scanning driven

accuracy. The accuracy of λ is controlled by the second-order partial derivatives' accuracy as derived from Eq. (2). Following the propagation of the elevation accuracy onto these parameters and the eigenvalues we obtain

$$m_\lambda = \pm \frac{\sqrt{6}}{d^2} m_z \quad (4)$$

With m_λ being the accuracy estimate of the eigenvalue, and m_z the laser elevation accuracy. Accounting also for surface roughness influence, a minimal detection level, ΔZ (minimal object response or detectable depth), is defined by the terrain's surface roughness, which relates to the eigenvalue computation via:

$$\lambda \approx \frac{2\Delta Z}{(d/2)^2} \quad (5)$$

Incorporating roughness and elevation accuracy, hypothesis tests that are formed for λ_{\min} and λ_{\max} for a confidence level, α , allow analysis of the response level. Consequently, instead of setting a unique threshold for the entire scene, each point is examined via its own z-test for a scale that can accommodate the first significant response. For gully analysis, the test is of the form

$$\frac{(\lambda_{\max} - \frac{2\Delta Z}{d^2})}{m_\lambda} > z_{1-\alpha} \Rightarrow \lambda_1 > z_{1-\alpha} \cdot m_\lambda + \frac{2\Delta Z}{d^2} \quad (6)$$

$$\frac{(\lambda_{\min} - 0)}{m_\lambda} \leq z_{1-\frac{\alpha}{2}} \Rightarrow |\lambda_2| \leq z_{1-\frac{\alpha}{2}} \cdot m_\lambda \quad (7)$$

with z , the normalized Gaussian distribution (Baruch and Filin, 2011).

4. Results

4.1. Fan characterization

Ze'elim — the laser scanning data reveal three zones in the fan surface (Fig. 4): i) an original Holocene fan (zone A in Fig. 4), consisting of coarse alluvial cobbles and pebbles and showing numerous stream channels, which form a braided stream pattern; ii) a transitional zone (zone B in Fig. 4), consisting of a thin veneer of fine grained alluvial cover deposited during the last 30 years on top of the silt-clay deposits of the recently exposed mudflat, and; iii) the distal part (zone C in Fig. 4), composed of a thick section of clay, forming at its eastern extension a steep slope that developed along the Holocene sub-lake distal part of the fan and deeply incised by numerous gullies that developed

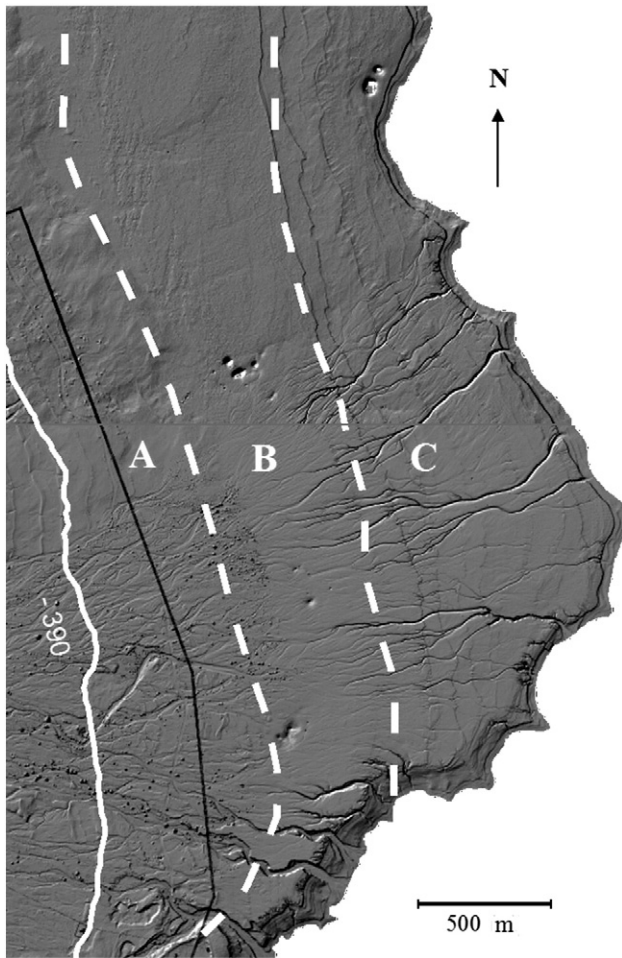


Fig. 4. Ze'elim alluvial fan — a shaded relief map derived from the laser scanning data. Three geological substrate and geomorphological development can be noticed: A — active fan composed of coarse gravels, and where shallow channels are developed; B — transition zone composed of thin alluvial gravels deposited on top of the mudflat, sinkholes and gully headcuts; C — mudflat exposed in front of the Ze'elim fan, abundant gullies and historical beachridges are present in this band. Black line crossing the fan is a power-line showing strong signature because of its relative height.

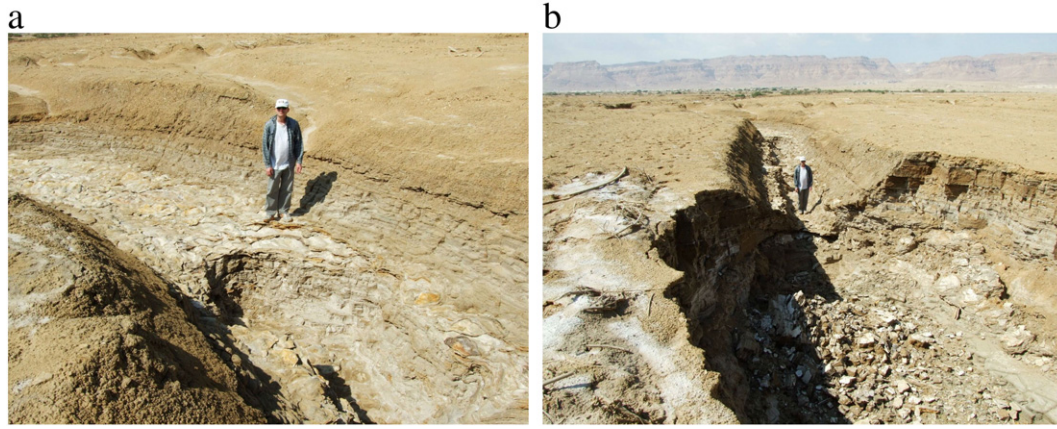


Fig. 5. Examples of knickpoint development along small scale gullies due to relatively resistant aragonite layers (Ze'elim fan). a) Small knickpoint. b) Large knickpoint.

over the last 30 yrs. This section exposes the Ze'elim Formation (Ken-Tor et al., 2001; Bookman et al., 2004; Bowman et al., 2007) that consists of fine-grain silt and clay with some interbedded aragonite layers. The aragonite forms relatively resistant layers, a few cm thick, that erode slower than the clay and silt layers, forming knickpoints within the relatively small gullies that dissect the Ze'elim Formation (Fig. 5). The newly exposed coastal zone is composed mainly of muddy-clay material, which originated in the fine-grained alluvial load. It was deposited at the distal part of the fans, while some of it was transported by the lake currents and spread in between the fans. The local annual lake retreat rate is readily traced by the distance between pairs of beachridges. The different zones can be distinguished by their roughness (RMS values of ± 10 , ± 5 , and ± 3 cm, using a 5×5 m² window size, for zones A, B, and C, respectively). The Holocene parts appear as rough surfaces that preserve the original geomorphic pattern of active channels and bars. The transition zones appear as smooth surfaces with low relief, locally disturbed by large collapse sinkholes. The distal parts appear as smooth surfaces incised by large dendritic linear gullies, well-defined shorelines, and embryonic sinkholes.

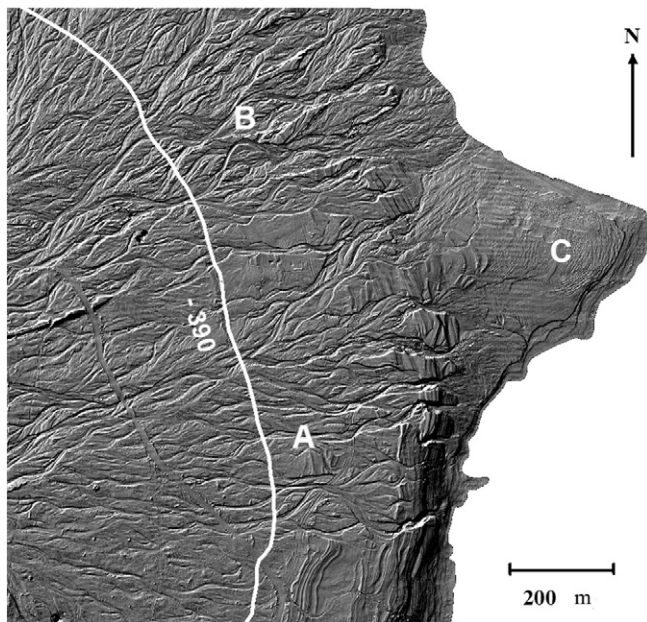


Fig. 6. Hever alluvial fan – a shaded relief map derived from the laser scanning data. Three zones with different patterns and roughness levels can be identified: A – old and inactive part; B – active part of the fan; and C – mudflat exposed in front of the coarse alluvial fan.

Hever – at present, the outlet of the active fan is located at the northern sector of the fan (zone B in Fig. 6). The southern sector of the fan (zone A in Fig. 6) which was abandoned ~30–40 years ago is characterized by a pattern of delicate braided channels and a smoother surface (RMS value ± 7 cm in zone A compared to ± 14 cm in zone B, both using a 5×5 m² window size) of fine-grained sediments and incipient development of soils. New mudflat exposure at the eastern tip of the active fan can also be seen in the eastern part (zone C in Fig. 6).

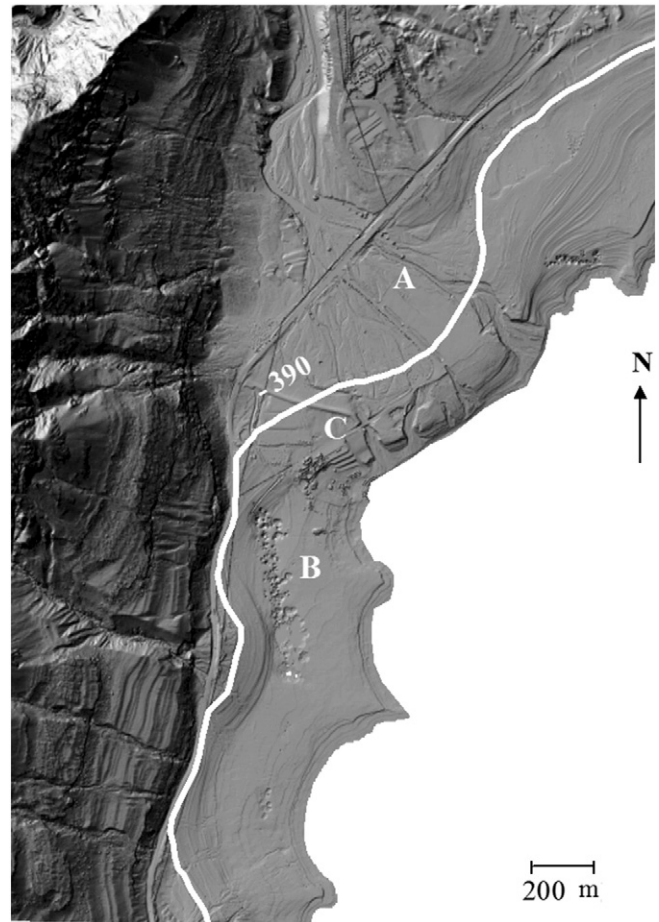


Fig. 7. Hazon alluvial fan – a shaded relief map derived from the laser scanning data. Three zones can be noticed: A – Hazon alluvial fan, dissected by four major channels; B – southern mudflat, penetrated by a dance cluster of sinkholes; and C – Mineral Beach resort.

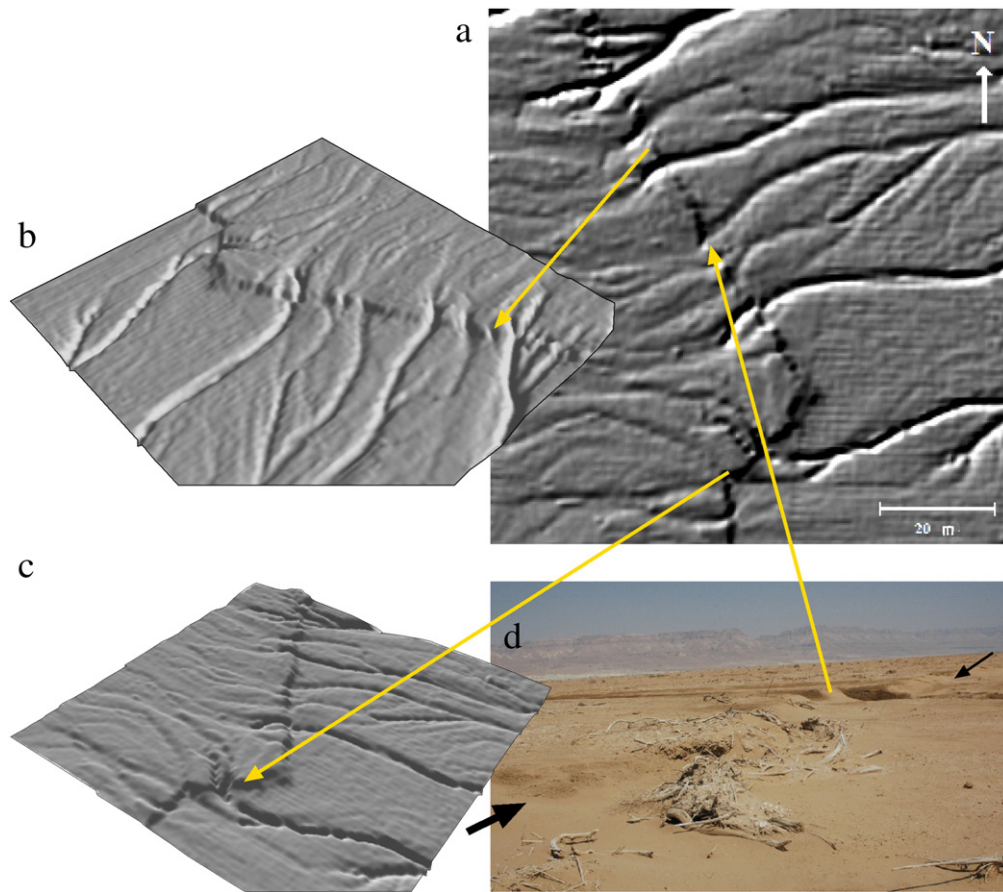


Fig. 8. Historical beachridges in the Ze'elim alluvial fan. a) Shaded relief derived from the laser scanning data. b) and c) Perspective views of extracts along the terraces derived from the laser scanning data. d) Image showing driftwood along the same beach terrace.

Hazon fan and Mineral Beach – four channels dissect the Holocene in response to the lake retreat of the past 25 years (zone A in Fig. 7). The mudflat, south of the fan, is clearly recognizable by its smooth surface (*RMS* value of ± 3 cm, using a 5×5 m² window size), on which a cluster of sinkholes is clearly noticeable. The Mineral Beach resort at the southern margin of the Hazon fan (zone C in Fig. 7) is endangered by the northward advancing sinkhole field on its south (zone B in Fig. 7), and by the deep incision of the Hazon stream channel on its north.

4.2. Beach ridges

Beach ridges reflect seasonal variations within the annual cycle of water level changes, in which winter receding rates are low (occasionally even rising), and summer rates are high. These ridges are commonly composed of pebbly, elongated ridges that were formed by high-energy wave impact during the high stands of the Dead Sea. Driftwood is commonly deposited on top of the ridges (Fig. 8d) and sometimes is even incorporated within them, especially on the upslope side (Bookman et al., 2004; Bowman et al., 2007).

A well-distinguished series of sub-parallel north–south shorelines cross the eastern part of the Ze'elim fan (Fig. 4). Fig. 8 shows the incision by gullies of such small ridges, which divert some of the fan's runoff towards the lake. Upon crossing the beachridges, the gully heads form a series of deep headcuts that migrate upstream, leaving behind deeply incised segments.

Correlating surface elevation data from laser scanning with lake levels, the beachridges are traced and associated with their year of formation (Fig. 9). As an example, a prominent ridge evolved during the

1991–1992 winter, when the lake level had risen by 2 m following an exceptionally rainy season (Figs. 8 and 9).

4.3. Sinkholes

Rapid sinkhole development along the coastal plains is one of the most prominent features that characterize geomorphic change in the study region. The sinkholes form because of the lake level drop that brings the subsurface fresh water to the level of the Holocene layer of salt, located at present about 20–50 m below surface. Fresh water that flows toward the lake dissolves the salt, creating unstable underground caverns onto which the alluvium above collapses. Sinkholes are commonly circular/oval shapes, ranging from ~1 m in diameter in their embryonic stage to several tens of meters when fully developed (Fig. 10). Occasionally the sinkholes are surrounded by conical collapse structures, followed by concentric cracks of sub-decimeter depth (Fig. 10). These concentric cracks, which develop around sub-surface caverns, appear before the collapse, and can serve as an early warning sign. In both regards, the resolving power of the laser scanning data is notable for distinguishing and locating them at the early stages of their development (Fig. 10; Filin et al., 2011).

Sinkholes appear in two types of host rock – gravel and mud. Morphometric analysis shows that in gravels the sinkholes are better preserved and are usually deeper (~6 m deep on average) and smaller in diameter than the mud type, which are ~1.5 m deep on average (Filin et al., 2011). We attribute this difference to a combination of two effects: i) mud sinkholes were formed in the distal part of the fan, where they are closer to the dissolving salt layer; and ii) following their initial development, the mud tends to collapse and fill the hole. Spatial relations

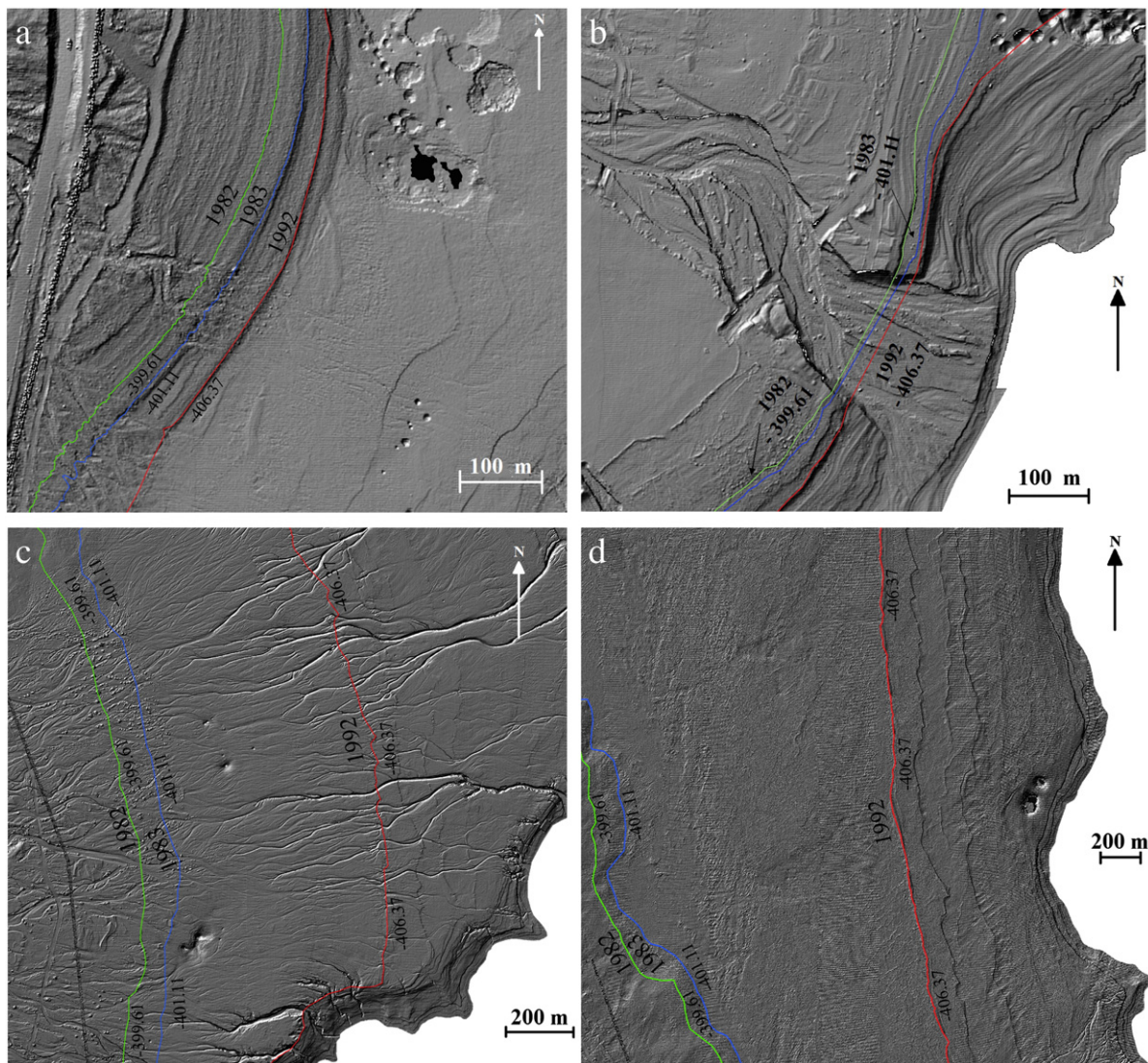


Fig. 9. Correlation of paleo-beach terraces with lake level records – the three contours reflect highly wet winters when substantial lake level rise has occurred. a) and b) Hazezon fan. c) and d) Ze'elim fan.

between embryonic sinkholes, small and shallow gullies, and delicate beach-terraces are presented in Fig. 11.

In the Hazezon, large sinkhole fields have developed on both sides of the fan. The largest and most hazardous developed along the southern border of the fan (zone B in Fig. 7). The elongate sinkhole field is oriented north-northwest, along a well-defined fault-controlled trend (Abelson et al., 2006) and is constantly propagating northwards towards the tourist resort and the Dead Sea highway.

4.4. Gullies and channels

We distinguish *gullies*, which develop rapidly in response to the lake level drop, especially in mudflats, and migrate upstream from the newly exposed beach (zone C in Fig. 4), from *stream channels*, which are wider, shallower, develop mainly at the outlets of the gravely fans and progress downstream aiming to reach the receding lake. The examples of the latter are found in Zone A in the Ze'elim (Fig. 4), Hever (Fig. 6) and Hazezon, (Fig. 7). During winter floods, gully headcuts migrate upstream at annual rates of tens to hundreds of meters (Avni et al., 2005; Ben Moshe et al., 2007; Bowman et al., 2010). Simultaneously, they expand towards the receding shore (Fig. 4). Their impact on soil erosion

and infrastructure makes them one of the main hazardous features in the Dead Sea region (Fig. 2).

The Hazezon Fan (Zone A in Fig. 7) is dissected by four major channels following the exposure of the steep slope in the distal part of the fan. South of the Hazezon fan, small gullies were developed on the mudflats (Fig. 11). These new gullies are relatively shallow (~30 cm) because of the limited flow generated from the small drainage basins (<1–2 km²). Some of these gullies flow towards sinkholes and have no outlet to the lake. North of the Mineral Beach, the main channels of the Hazezon incise the Holocene gravely fan. These channels show slight widening near their outlet to the lake. As the lake shrinks, the channels propagate towards the receding shores. This propagation is evolving simultaneously with the deepening of the channels accompanied by widening by bank collapses during or shortly after flood events (Bowman et al., 2010).

In the Hever fan (Fig. 6), small stream channels have been developing in the southern, inactive, sector of the fan. They develop due to the exposure of steep slopes in the proximate sector of the fan. These small stream channels are not connected to the main channel on the Hever fan and are fed only by local showers that generate rare local flash flows.

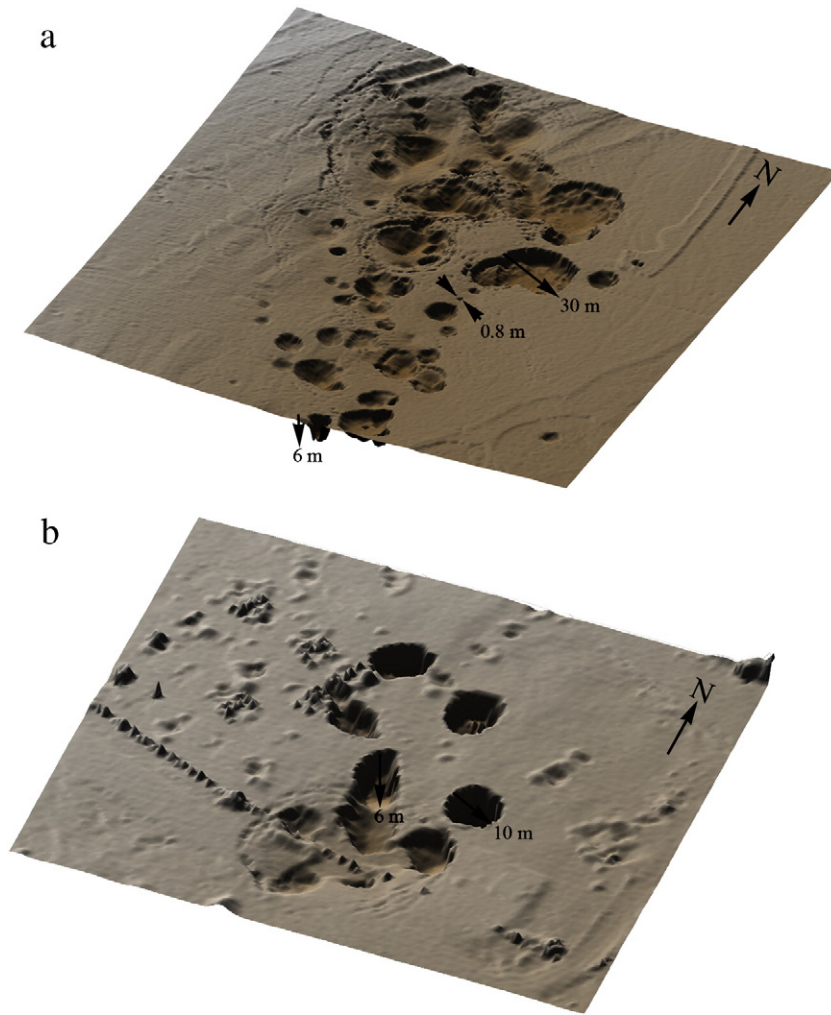


Fig. 10. Sinkholes expressed in the laser scanning data for two locations. a) Sub-meter collapse as well as concentric fractures, which indicate the dynamic nature of the process. b) Mature wide and deep sinkholes characterized by sharp elevation drop.

Numerous gullies dissect the Ze'elim fan, flowing eastward. These gullies are relatively narrow and their banks consist of almost vertical walls (Fig. 4 and 12). They are up to 6 m deep and 10 m wide, becoming wider and well-defined as a result of the convergence of several tributaries. An additional contribution to the increasing dimensions in some segments of the gullies is the collapse of steep gully side walls (Fig. 12), especially in places where the local ground water table is exposed by deep gullies.

The section of the Ze'elim Formation exposed by the gullies is rather homogeneous, composed mainly of silt and clay interbedded with some layers of relatively hard argonitic crusts that can make hard zones in the strata (Ken-Tor et al., 2001; Bookman et al., 2004; Bowman et al., 2007). When these hard aragonite layers are exposed during the general down-cutting by the relatively small gullies (<500 m in length), they can form distinct knickpoints that are gradually migrating upstream as a function of the flood pulses (Fig. 5).

Headcuts developed on the upstream segment of the gullies between the thalweg and the fan surface (Fig. 12c) form a near vertical drop, up to 3.5 m deep. The shallow channels that flow towards the gully headcuts are 2–4 m wide and 0.2–0.4 m deep, with relatively flat bottoms and no knickpoints. These shallow channels transport the unconfined flow from the gravelly fan toward the mudflat (Zone B in Fig. 6). The shallow channels are trapped by the gully headcuts, which in turn use their flow for migrating upstream.

4.5. Analysis of channel and gully geometry

We analyze stream channels and gullies that have been developing in two sedimentary environments: gravel fans and mudflats.

Stream channels within gravel fans (Hazezon fan) – occasional flow generated from the Hazezon basin is directed into several main channels, among which the northern one is the largest (Fig. 13a). The upstream segment (from highway 90 in the west towards the channel's outlet) is ~300 m long, relatively straight, 12–15 m wide, and 2–6 m deep. The downstream segment is wider because of a meander that propagates northwards. The 55–60 m wide channel bottom is characterized by a rough micro-topography due to residual terraces, which have been developing along the flow paths sorting coarse gravels (Fig. 13c,d). The banks above the main channel are 6–10 m high. The smooth longitudinal section along the active channel (Fig. 13b) indicates near equilibrium relations between the lake level drop and the incision along the main channel. The near equilibrium has been reached and maintained over the last 15 years.

Gullies within mudflat surfaces (Ze'elim) – most of the Ze'elim gullies developed in the distal part of the large exposed fan in the muddy Holocene Ze'elim Formation (Bookman et al., 2004). Fig. 14 shows such an example, focusing on the main gully path and two of its tributaries. Using the laser data, both thalweg profile and a dense set of cross sections along both the main gully and branches are extracted and

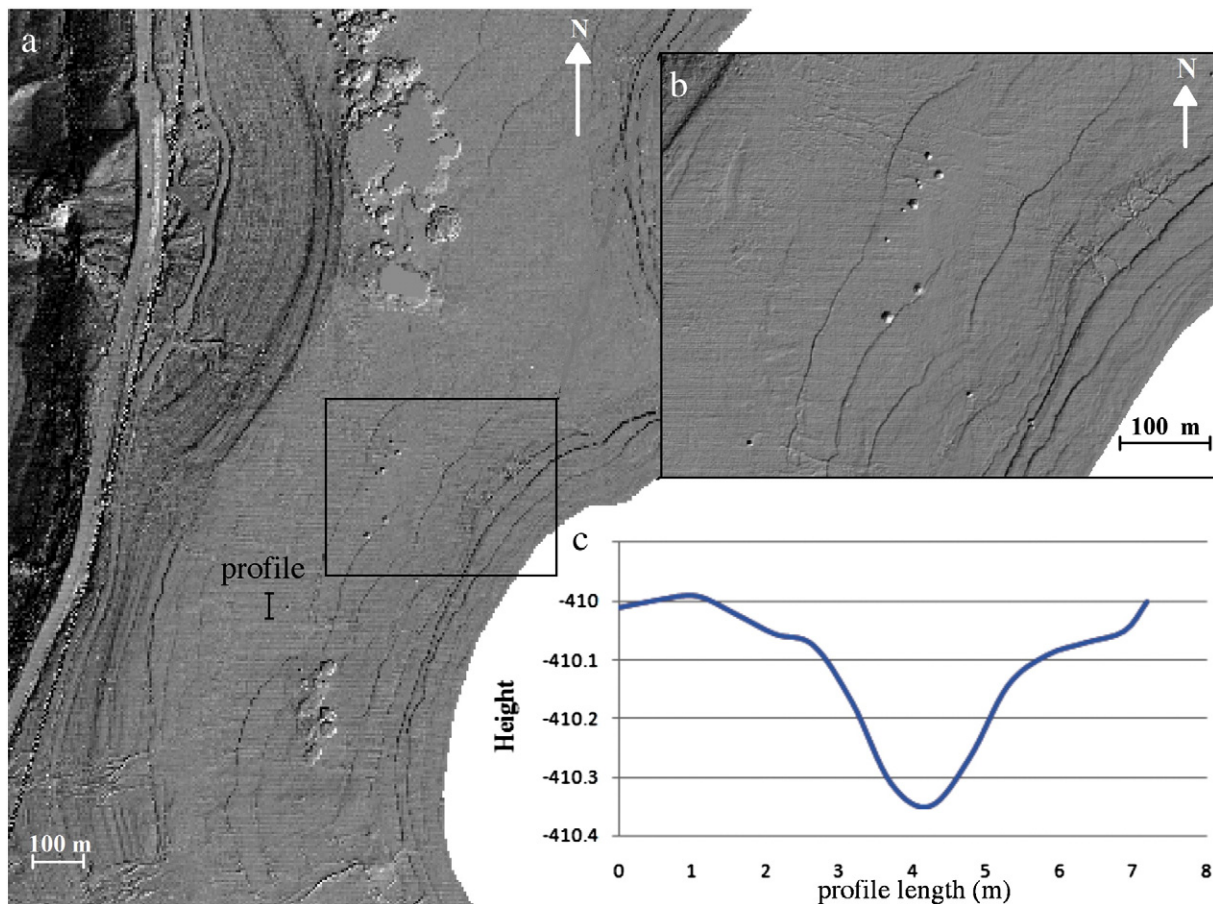


Fig. 11. Shallow sinkholes developed on the mudflat of Mineral Beach. a) A laser scanning derived shaded relief images of the mudflat south of the Mineral Beach campsite with a major sinkhole field in an NNW direction. b) Enlargement shows the location of an embryonic sinkholes field. c) The relations with a 30-cm-deep gully and a sinkhole are illustrated.

assessed, comparatively. Fig. 14b reveals the incision process that this gully has been undergoing. Several knickpoints along its profile can be observed, with the rightmost featuring the gully's headcut.

Another section along the gully profile (S4 in Fig. 14) reflects the more substantial incision, which adapts to lower lake levels and begins as the receding lakeshore reaches the distal part of the fan, where the slope is steeper (Fig. 14). After its initiation, the development of the gully is influenced by two forces: i) the receding lake, driving its downstream elongation, and ii) headward propagation of the upper headcut and some inner knickpoints. This 'dual' incision is shaping an almost linear dynamic feature and the integration of several parallel gullies shape a dendritic pattern, connecting the distal part of the active fan with the receding lake. The concave profile of the gully in its lower part is a result of ground water seepage exposed in the bottom of the gully and causes large slumps (Fig. 12). The sharp elevation drop in this composite headcut (Fig. 12) drains the surface flow generated by the braided shallow channels in that part. The 1–2 m drop during flow events is sufficient to trigger migration of the headcuts upstream.

Cross-section stacking of both the main gully and branches (Fig. 14c) shows their simultaneous widening and deepening. The gullies and branches develop at the same pace and have similar shape. In addition to transport of eroded material, the widening also occurs by substantial sidewall collapse during or shortly after the floods. Deepening is mainly developed by action of knickpoints and headcut migration initiated by several mechanisms, including the breaching of beach ridges (Figs. 2e and 8) and the exposure of resistant layers within the incised section (Fig. 5). In addition, the impact of rare events of lake level rise (e.g. 1991–1992) that shape steep coastal steps, can trigger the development of new headcut and gullies (e.g., Fig. 14a).

Another example is given by an almost linear gully (Fig. 15) which bears a few branching tributaries incised in an almost flat surface. The thalweg and bank profiles (Fig. 15b) are indicative of the incision process. The thalweg is rather flat with very few knickpoints along the profile. The small tributary (B2 in Fig. 15a) joining the main gully (B1) in a steep knickpoint (F1), reflects the lack of flow power in this tributary due to its small drainage area. Fig. 15c shows a stacking of cross-sections of both the main gully and branches. The most important observation, made possible by the laser scanning data, is that despite major differences in length and flow between the two gullies, B1 and B2, they share similar shape and geomorphic characteristics. This indicates that the most important factor controlling the shape of the gullies developed in the recently exposed zone is the erodibility of the substrate in which the gullies are incised, which is the almost homogeneous clay and mud composing the mudflats.

One of the shortest gullies in the Ze'elim fan (Fig. 16) is only 500 m long, compared to the ~1000 to 1200 m length of gullies shown in Figs. 14 and 15. The gully is located along one of the steepest sectors of the exposed distal part of the fan. It is divided into three segments: the relatively shallow western segment (left side), the deeply incised central segment and the eastern outlet of the gully toward the receding lake. This segmentation is demonstrated in Fig. 16b, which reveals the deep incision of the central segment and the sharp drop in elevation both in the entrance to the gully and its outlet, characterized by the development of several small-scale knickpoints. The general configuration strongly demonstrates the combined influence of the sharp topography of the fan edge, generating high erosion potential, with small flow in this drainage basin, which limits the ability of the gully to incise in spite of the high potential. Fig. 16c shows a stacking of cross-sections

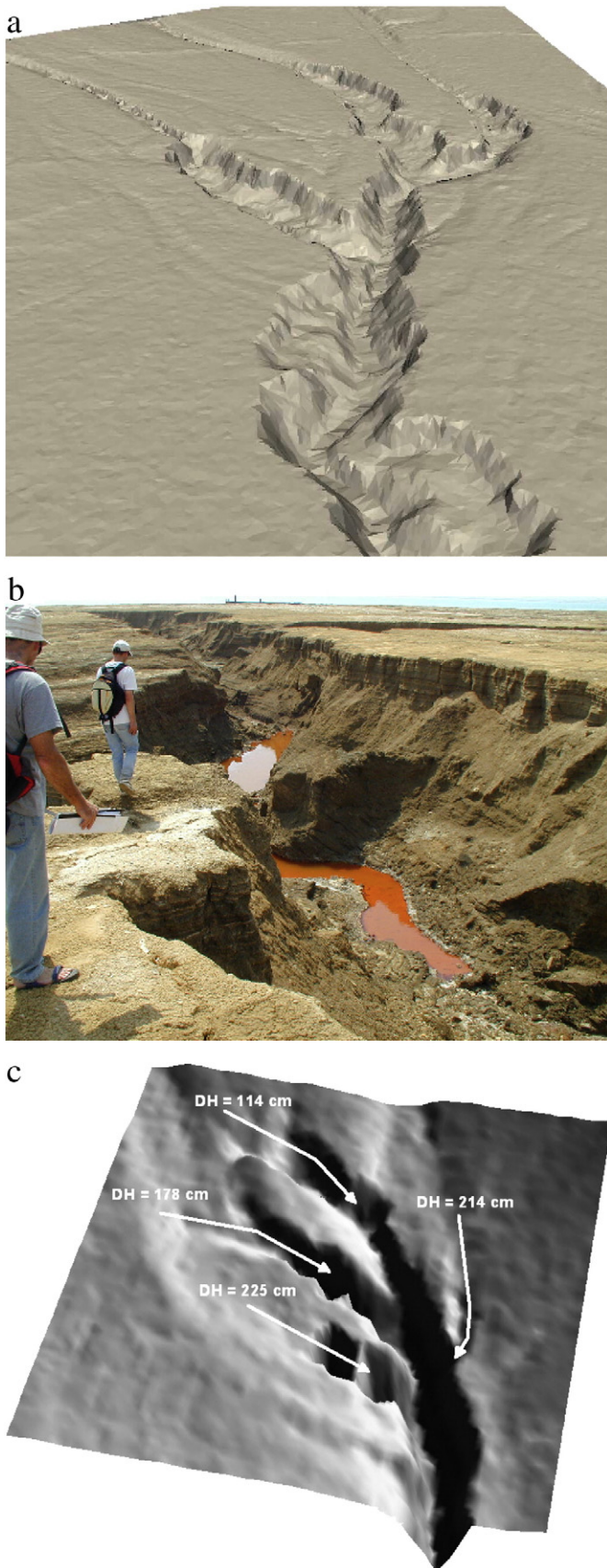


Fig. 12. Newly incised gullies on the Ze'elim fan. a) Laser scanning derived perspective view of a gully that started to form in the mid 1990s. b) Ground water seepage flow along the channel and causing large slumps. c) Perspective illustration showing knickpoints.

of the main gully. Most of the drainage into this gully is blocked by the combined effect of rapid development of the nearby gullies and a large sinkhole field that forms a prominent depression (Fig. 4). Both features attract the surface flow and hinder further geomorphic development of this gully.

4.6. Total sediment erosion

Three-dimensional characterization and quantification of the total volume of the fan's surface and the alluvial sediment eroded by the gullies can be estimated directly from the data. Surface volume is directly computed by integrating the fan surface topography, and for the channels and gullies, following their delineation, via summation of a sequence of prismoid volumes

$$v = \sum_{i=1,3,5}^{n-2} 2h \frac{S_i + 4S_{i+1} + S_{i+2}}{6} \quad (7)$$

with v being the eroded volume, S_i the area of the i -th prismoid bases (bottom, intermediate, and top), and h the prismoid height. The prismoid bases are profiles extracted across the channel path, where the interval between them (dictating the height) dictates the resolution of the computation.

Volumetric sediment erosion computations are presented for the Hazezon and the Ze'elim fans (Table 1). The total calculated volume of the Hazezon fan before incision is $1.0 \times 10^7 \text{ m}^3$, which was computed by depth integration over the fan area. As there is no simple way to calculate the thickness of the buried part of the fan, it was approximated using an average incision into the fan by the gullies. Over the past 25 years the channels removed $\sim 9.6 \times 10^4 \text{ m}^3$ of gravels, which are 0.96% of the total fan volume. The mean annual sediment removal rate is estimated at $3.8 \times 10^3 \text{ m}^3 \text{ y}^{-1}$. The total calculated volume of the Ze'elim fan before the incision was $\sim 5.7 \times 10^7 \text{ m}^3$ while the total gully volume which has incised in the fan during the last 25 years is $\sim 3.3 \times 10^5 \text{ m}^3$, which are 0.57% of the original fan. The mean annual sediment removal rate is estimated at $1.3 \times 10^4 \text{ m}^3 \text{ y}^{-1}$.

5. Discussion

5.1. Morphological zones of alluvial fans

The flow toward the Dead Sea from the outlet of the drainage basins is segmented into several fluvial zones with different morphological characteristics, best demonstrated at the Ze'elim and Hever fans (Figs. 4 and 6). A single fluvial stream channel is developed in the western sector of each one of these basins, connecting the outlets of the deep rocky gorges with the alluvial fans in the Dead Sea coastal strip. These late Pleistocene fans, which were developed when Lake Lisan occupied the Dead Sea basin, are deeply incised (Begin et al., 1974). As the Ze'elim stream channel reaches the eastern edge of the Pleistocene fan, it opens to form the present (Holocene) alluvial fan which is composed of coarse alluvial gravels. This zone developed a set of shallow braided channels that spread boulders and cobbles throughout the fan (A in Fig. 4). The recently-exposed area (the third zone) is almost bare and rather smooth ($RMS \pm 5 \text{ cm}$) without localized drainage structures (B in Fig. 4). As the shallow flow migrates eastward toward the Dead Sea, a series of gullies takes over, forming prominent headcuts at the very beginning of the gullies (C in Fig. 4). Finally, well-incised gullies, dissecting the mud flats, develop (C in Fig. 4). Within most of the relatively small gullies, some inner knickpoints are developed. Large-scale slides also develop due to drying up of the exposed section after floods and the exposure of the local ground water at distinct locations below the incised fan. When the gullies approach the lake, they become shallower as a function of the small vertical interval between the gully outlet and the continuously receding lake.

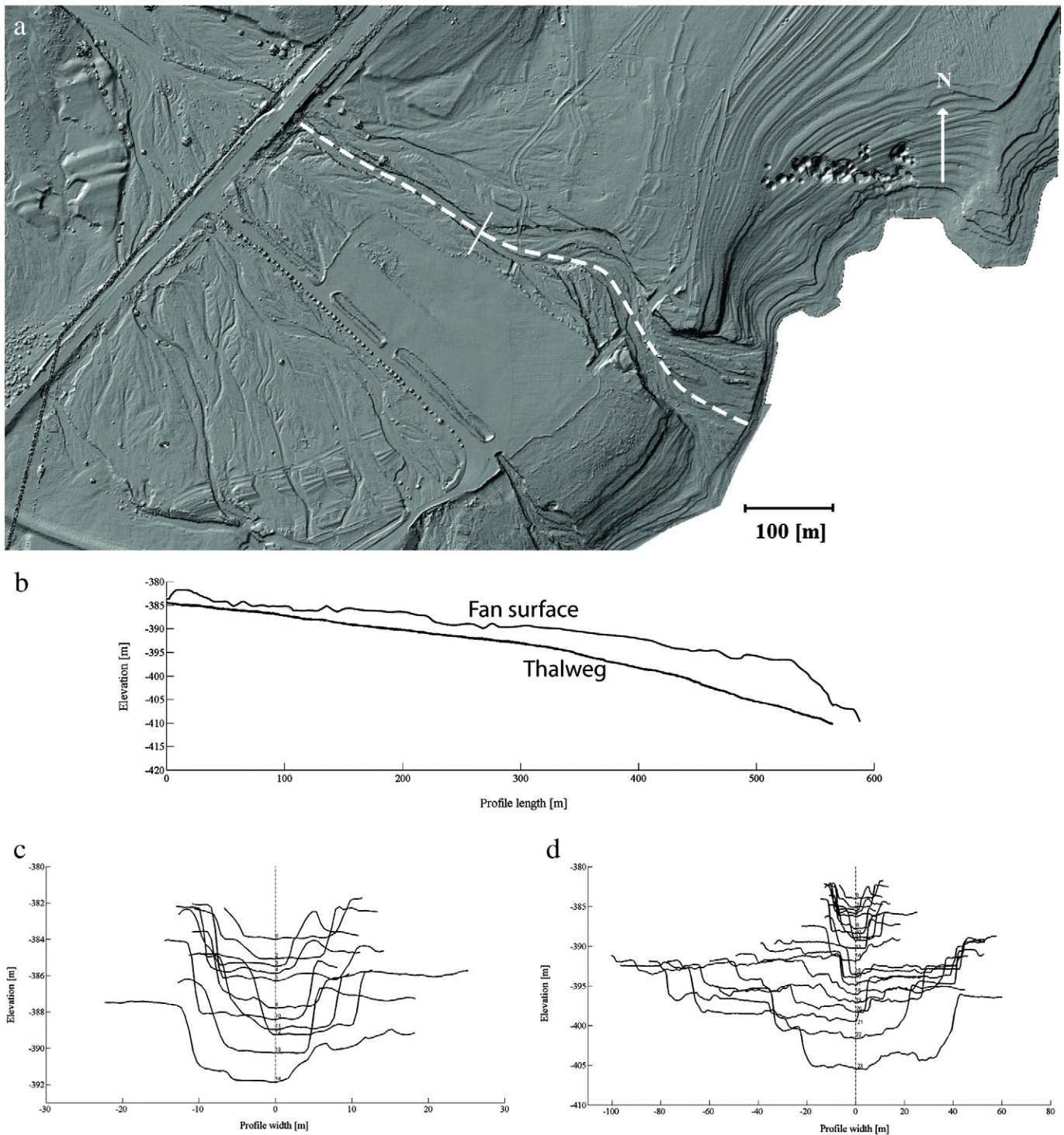


Fig. 13. Incision along the Hazezon Wadi. a) Shaded relief map showing topography and the location of the profile section (dashed). b) Longitudinal profile along the thalweg. c) Cross sections of the upper part of the thalweg (from the thalweg head to the marked tick in 'a'). d) Cross sections of the upper part of the thalweg (from the marked tick in 'a' and downstream).

The common fluvial structure in coarse and gravelly terrain is wide, and shallow stream channels form a braided pattern (A in Fig. 4 and A and B in Fig. 6). No knickpoints were observed in this sector, and its thalweg profiles are rather smooth. However, where the alluvial substrate is fine grained, the typical drainage pattern is characterized by linear well-incised form with steep banks and some knickpoints along it. Therefore, we conclude that the type of the substrate and the dimensions of the fluvial features control the fluvial pattern which was developed along the Dead Sea shore.

5.2. Connectivity of the fluvial system

As the lake-level drops and the coastal zone expands, the braided stream channels propagate downstream, preserving their braided pattern (A and B in Fig. 6). At the distal parts of the exposed alluvial fans the flow disperses in the mudflats and migrates eastward into the lake. Simultaneously, the gullies that gradually migrate upstream, trap the unconfined flow, which is then confined within the gullies. As the gullies migrate upstream toward the fans they bridge the gap between

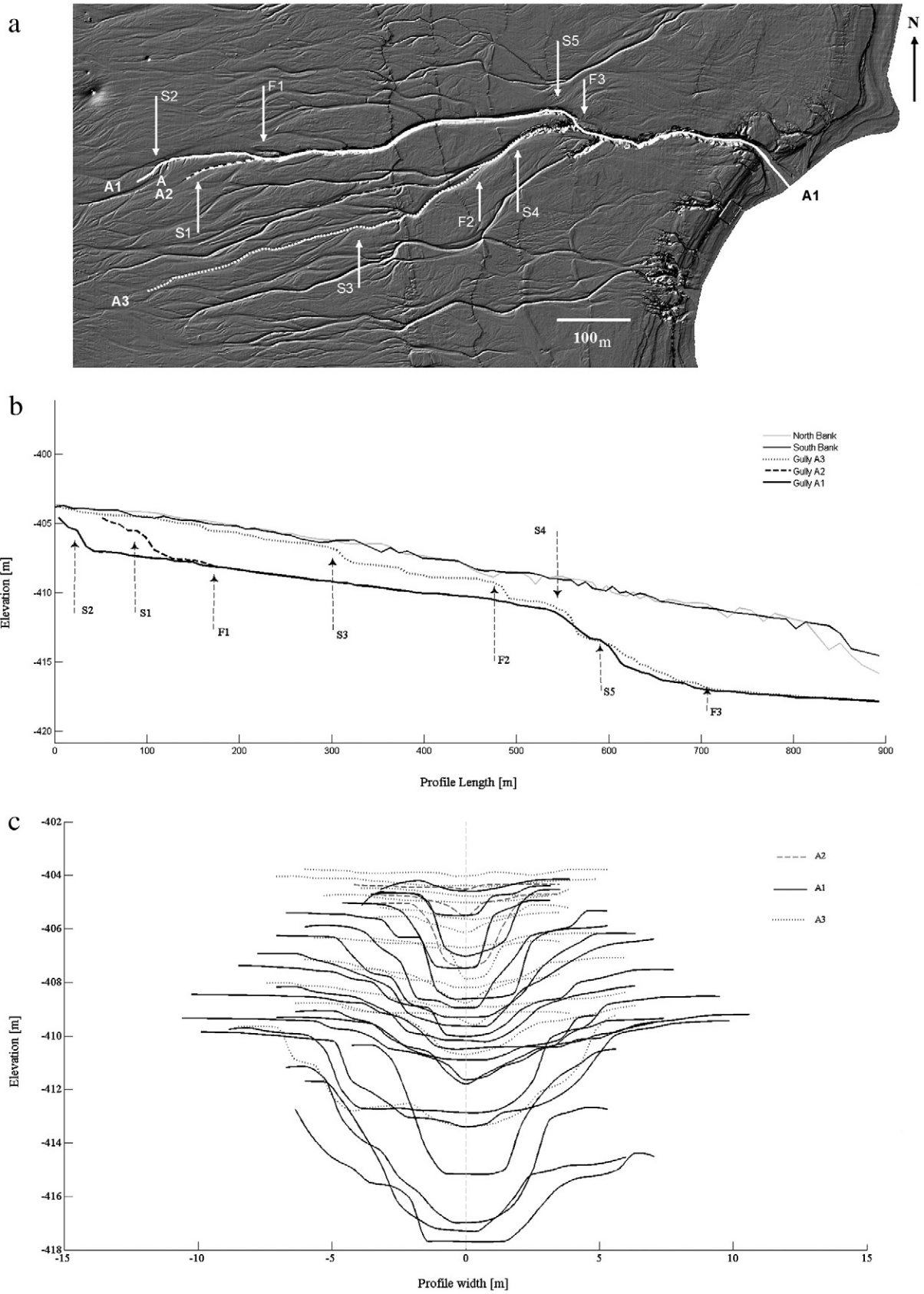


Fig. 14. Gully incision at the northern part of Ze'elim alluvial fan. a) Gully dissecting the mudflat with two of its tributaries. Key points along it are marked. b) Longitudinal profiles of the thalweg and its two tributaries. c) Cross sections along the channel and its two branches.

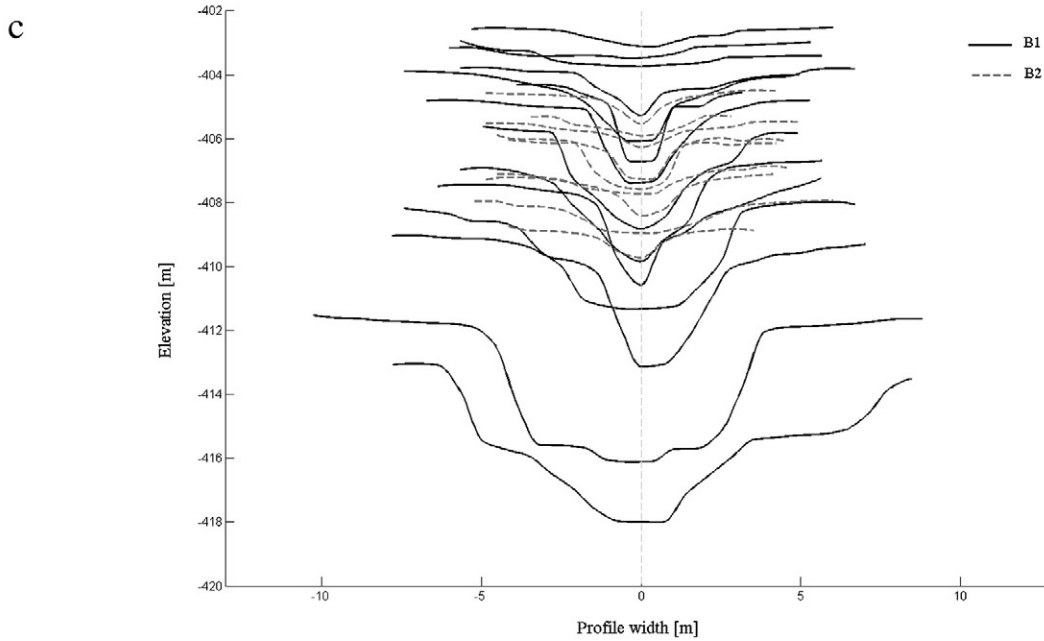
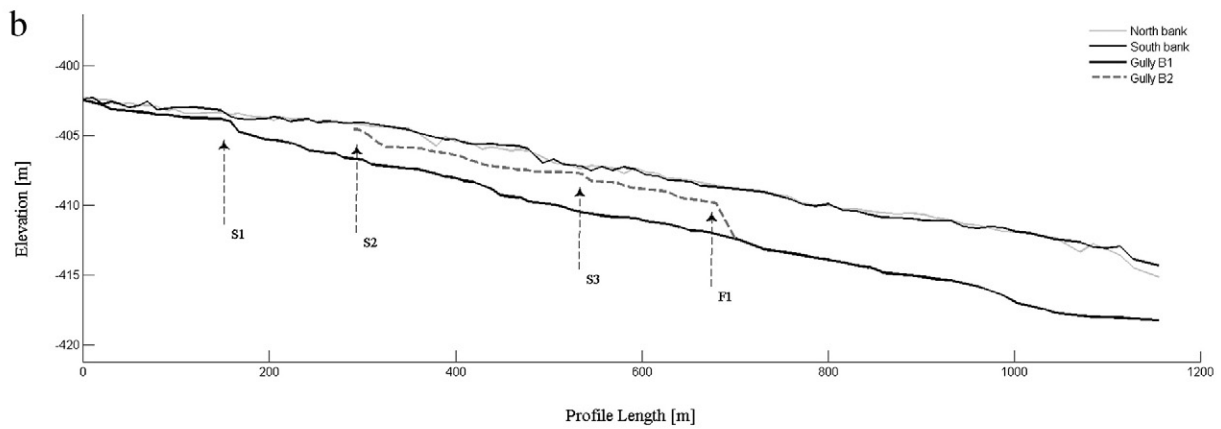
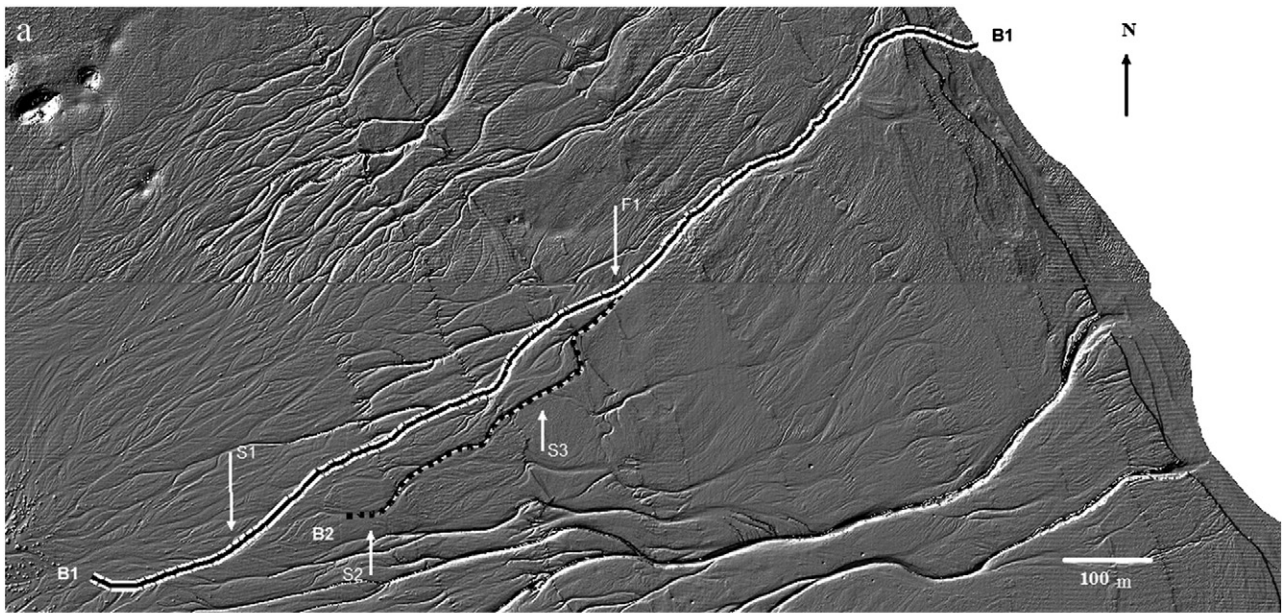


Fig. 15. Gully incision at the central section of Ze'elim alluvial fan. a) Gully dissecting the mudflat with one of its branches. Key points along it are marked. b) Longitudinal profiles of the thalweg and its tributary. c) Cross sections along the channel and a tributary.

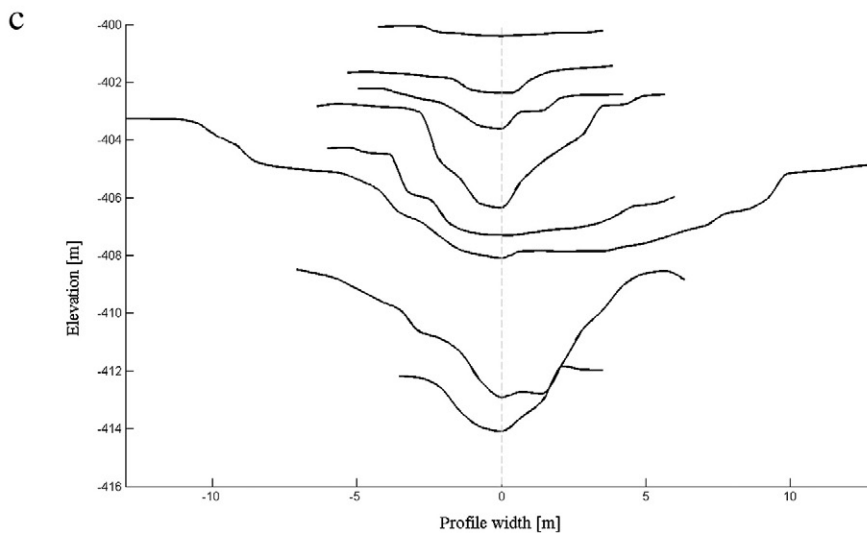
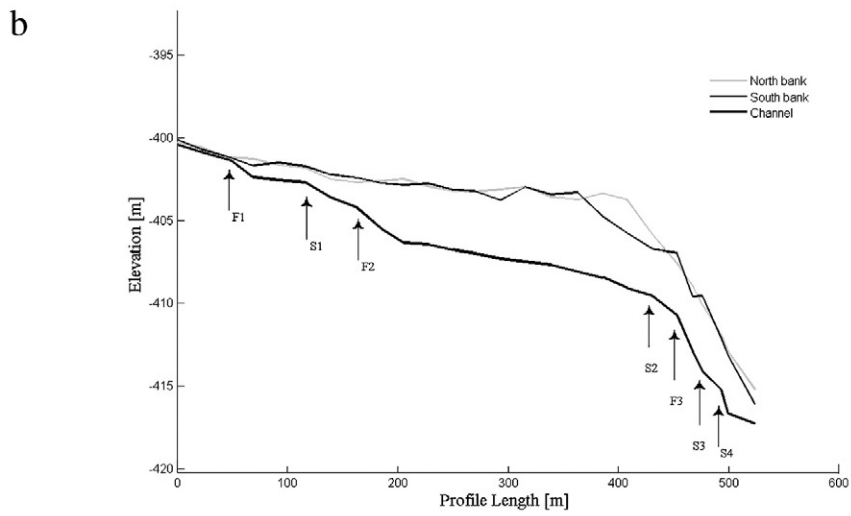
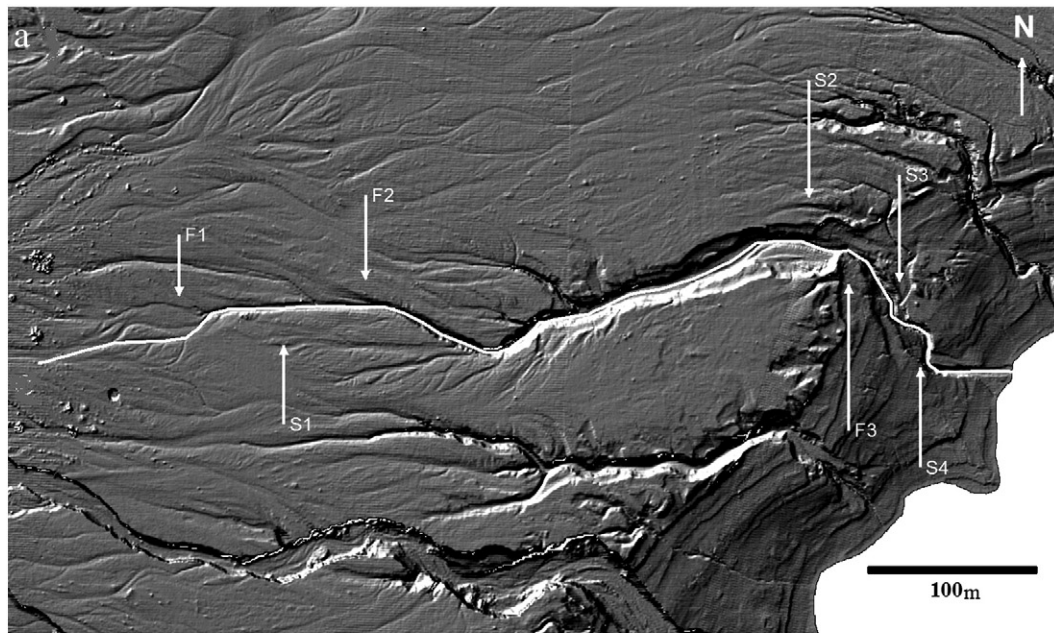


Fig. 16. Gully incision at the southern part of Ze'elim alluvial fan. a) One of the shortest gullies dissecting the Ze'elim mudflat, located in its southern part. b) Longitudinal profiles of gully 10 thalweg and banks. c) Cross section of gully10 thalweg and banks.

Table 1

Comparison between the erosion rates and total removal of geological substrate by the Ze'elim gullies and the Hazezon stream channels.

Site location	Ze'elim	Hazezon
Geological substrate	Clay and fine grained alluvium	Fluvial gravels
Total volume of alluvial fan	$5.7 \times 10^7 \text{ m}^3$	$1.0 \times 10^7 \text{ m}^3$
Total channel erosion during the last 25 years	$3.3 \times 10^5 \text{ m}^3$	$9.6 \times 10^4 \text{ m}^3$
Percentage of total eroded material	0.57%	0.96%
Annual erosion rate	$1.3 \times 10^4 \text{ m}^3 \text{ y}^{-1}$	$3.8 \times 10^3 \text{ m}^3 \text{ y}^{-1}$

the lake and the fan. Therefore, most of the gullies can be considered as the extension of drainage streams. This is especially true in the Dead Sea region, where the hyper arid climate minimizes the flow from local sources, such as from hillslopes or from areas in the coastal zone that are located in between the fans.

The gullies originate where the gradient is the steepest (Fig. 16; Bowman et al., 2011) and develop simultaneously downstream toward the lake as the level drops, and upstream, as the headcut gradually migrates toward the headwater. This upstream migration is a function of the amount of concentrated flow in the specific gully, the stream power, and the erodibility of the substrate at the headcut. This headcut migration can be rapid in mud but much slower in coarse gravels (Begin, 1987; Ben Moshe et al., 2007). As this process continues, the upstream headcut propagation connects with the stream channels in the alluvial fans (Bowman et al., 2011). This scenario, which is rare at present, will lead to high connectivity of the fluvial system along the Dead Sea coastal zone and to increased incision along major gullies, while others gullies will become depleted of flow water.

5.3. Longitudinal profiles

The ongoing lake level drop facilitates the incision of channels and gullies. The questions that arise are whether the incision is continuous

or episodic and whether a near equilibrium can be achieved in this rapidly changing environment.

The Dead Sea is characterized by almost constant base level drop reaching $1\text{--}1.3 \text{ m y}^{-1}$, a few (1–4) powerful winter floods, and relatively homogeneous substrate. Under these conditions rapid adjustment of the longitudinal profile of the larger gullies and channels has been observed (Hassan and Klein, 2002; Bowman et al., 2007, 2010). Additionally, these studies reported no knickpoint development in muddy sediments and in the coarser gravelly material (Bowman et al., 2007).

We differentiate stream channels and large gullies from small scale gullies. We argue that near equilibrium is reached only along the stream channels and large gullies, which attract the large portion of the flood water. Near equilibrium is reached because of the flood energy which is more powerful than the substrate resistance. Under these conditions, equilibrium is reflected by their almost straight and smooth thalweg profile (Fig. 13b). However, small scale gullies attract a smaller portion of the flood water, therefore they are more influenced by the variation in the substrate (e.g. aragonite layers, Fig. 5) and topography. These factors account for the development of knickpoints along the thalweg (e.g., Figs. 14 to 16).

Embryonic gullies and headcuts develop when the lake level drop exposes steep slopes of the former bathymetry (such as the distal fan slope in the eastern sector of the Ze'elim fan). Another cause of headcuts and knickpoint generation is a result of relatively resistant aragonite layers exposed within the Ze'elim Formation (Ken-Tor et al., 2001; Bookman et al., 2004; see Fig. 5). As these hard layers are rare in the section and rather thin, their impact on the general longitudinal profile in most of the large gullies is of short duration. However, low velocity and low frequency floods are essential for the long survival of these knickpoints in the gully bottoms and they control the general shape and longitudinal profile of the smaller gullies for a longer time.

Another mechanism for gully and headcut formation occurs during the rare episodes of lake level rise, which form prominent coastal cliffs due to the wave impact on the soft, fine grained alluvium or distinct beach ridges on low inclined surfaces. This is the case of the lake level rise in 1992–1994 (Fig. 1c), which formed distinct coastal cliffs of

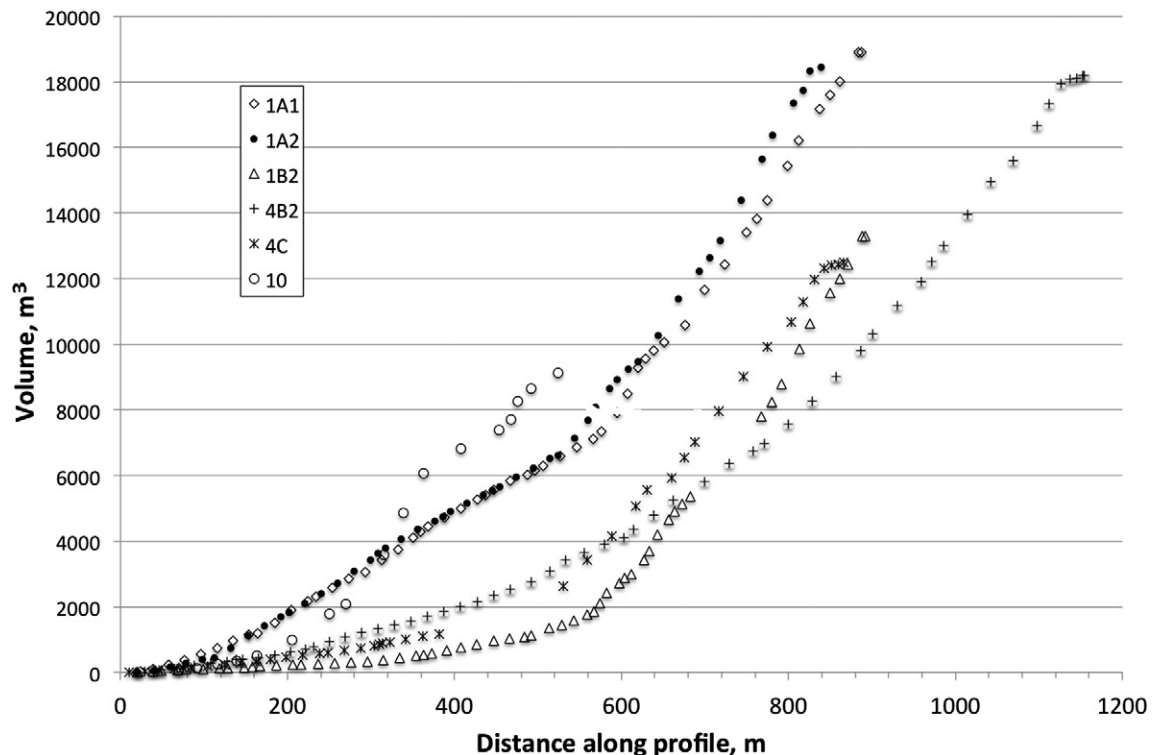


Fig. 17. Volume of incised gullies along their length. Similar slope is attained about 550 m from the shore.

approximately 2 m. The distinct beach ridge on the Ze'elim mud flat (Fig. 8) forced the unchanneled flow to accumulate behind it (Bowman et al., 2011), until it reached a critical level and breached the obstacle. This process generates an upper headcut in some relatively small gullies as indicated in Figs. 8, 9c and 12. The upper headcut developed due to the relatively high topographic gradient facilitated by the downslope side of the beach ridge. After its initiation, the headcut migrated upstream.

The cross sections (Figs. 14c, 15c and 16c) indicate that the gullies become deeper and wider simultaneously (Figs. 14 to 16). The flat sections between steps where bottom gradients are in the range of 0.6–1.2% appear to be in near equilibrium for relatively short time intervals.

Plotting the volume of eroded material along the profiles (Fig. 17) we observe a tendency toward uniform slopes, suggesting the dynamic equilibrium rate of erosion. Nevertheless, precise estimation of erosion rates should be obtained by comparing two scans from different times.

5.4. The fluvial network vs. laboratory simulations

Most of the stream channels developed in the alluvial fans and the gullies developed in mudflats along the Dead Sea coastal zone have similar shape and geomorphic characteristics. This indicates that the most important factor controlling their shape is the erodibility of the substrate in which the channels develop. In this regard, the present gully pattern developed along the Dead Sea coastal zone (Figs. 14 to 16) is very similar in shape to those developed in flume experiments on a homogeneous substrate of clay and mud (e.g., Begin et al., 1981; Koss et al., 1994). Therefore, the fluvial and other geomorphic processes developed during the last decades in the Dead Sea region can serve as a natural large-scale analog site for these experiments. It can serve as a validation site for a large variety of geomorphic and geologic processes such as the influence of base level lowering on the geomorphic system (Horton, 1945; Mayer, 1990; Bowman et al., 2010) and for sequence stratigraphy in lakes and rivers (Schumm, 1993).

As the annual precipitation in the Dead Sea basin is ~50 mm, most of the gully-generating flow is supplied by the main stream of Wadi Ze'elim through its alluvial fan. Therefore the gullies are elongated with only a few branching tributaries. This pattern differs from ones developed in humid environments, which exhibit badlands morphology with several side tributaries merging into the main gullies (Campbell, 1989).

6. Conclusions

The laser scanning technology enables us to detect sub-metric features, such as narrow and shallow channels and gullies, beach ridges, small headcuts, and embryonic sinkholes. Combined with the accurate location of these features, it is of prime importance in describing and formulating the environmental changes and hazards in active regions. The ability to compute 3D properties of geomorphic features is a powerful tool for quantifying soil loss, volume, erosion, and growth rates of gullies, headcuts, and sinkhole fields, which are endangering the natural environment and infrastructures.

We show that gullies begin to develop as soon as a new surface is exposed, especially after the formerly submerged distal part of the alluvial fan, characterized by steep slopes, was exposed, and that the gullies become wider and deeper simultaneously. In a few years' time large parts of the gullies' bottom reach a stable slope of 0.6–1.2%, which is maintained between knickpoints. The knickpoints are formed by the combined effect of relatively resistant aragonite-rich layers within the more common clay beds.

The present study focused on the Dead Sea region, which is representative of active, rapid geomorphic and environmental changes. Most of the active features described along the Dead Sea coast are known also in other regions on Earth, in particular lakes that are

under the warming trend. Therefore, the Dead Sea region can serve as a natural laboratory for experiments and a validation site for a large variety of geological and geomorphological processes, including flume experiments in extreme arid environments. We realize that the incision has affected mostly the mudflats and has reached the boundary zone between the mudflats and the coarse alluvial surface of the fans only recently. It is therefore impossible to infer from the current transient state how the incision will behave in other types of surfaces. Nevertheless, more precise estimation of future fluvial patterns and erosion rates should be obtained by comparing two scans from different times.

Acknowledgments

The research was funded in part by grants provided by the Israel Ministry of Science through the Dead Sea and Arava Science Center, the Israel Ministry of National Infrastructure, the Henri Gutwirth Fund for the Promotion of Research, the Geological Survey of Israel, Bank Ha'poalim endowment fund, and an Israel Science Foundation grant 1539/08 to S. Marco. Special thanks are expressed to YakovRefael and Hallel Luzki, the Geological Survey of Israel, for technical assistance.

References

- Abelson, M., Yechieli, Y., Crouvi, O., Baer, G., Wachs, D., Bein, A., Shtivelman, V., 2006. Evolution of the Dead Sea sinkholes. In: Enzel, Y., Agnon, A., Stein, M. (Eds.), *New frontiers in Dead Sea paleoenvironmental research*. Geological Society of America Special Paper, 401, pp. 241–253.
- Akel, N., Filin, S., Doytsher, Y., 2007. Orthogonal polynomials supported by region growing segmentation for the extraction of terrain from LiDAR Data. *PE&RS* 73, 1253–1266.
- Avni, Y., Zilberman, E., Shirav, M., Katz, O., Ben Moshe, L., 2005. Response of the geomorphic systems along the western coast of the Dead Sea to sea level lowering and its implications on infrastructure. Report GSI/18/04.
- Baruch, A., Filin, S., 2011. Detection of gullies in roughly textured terrain. *ISPRS J. Photogramm. Remote Sens.* 66, 564–578.
- Begin, Z.B., 1987. Application of a diffusion-erosion model to alluvial channels which degrade due to base-level lowering. *Earth Surf. Process. Landf.* 13, 487–500.
- Begin, Z.B., Ehrlich, A., Nathan, Y., 1974. Lake Lisan, the Pleistocene precursor of the Dead Sea. *Geol. Surv. Isr. Bull.* 63 (30 pp.).
- Begin, Z.B., Meyer, D.F., Schumm, S.A., 1981. Development of longitudinal profiles of alluvial channels in response to base-level lowering. *Earth Surf. Process. Landf.* 6, 49–68.
- Ben Moshe, L., Haviv, I., Enzel, Y., Zilberman, E., Matmon, A., 2007. Incision of alluvial channels in response to continuous base level fall: field characterization, modeling and validation along the Dead Sea. *Geomorphology* 93, 524–536.
- Bookman, R., Enzel, Y., Agnon, A., Stein, M., 2004. Late Holocene lake levels of the Dead Sea. *Bull. Geol. Soc. Am.* 116, 555–571.
- Bowman, D., Shachnovich-Firtel, Y., Devora, S., 2007. Stream channel convexity induced by continuous base level lowering, the Dead Sea, Israel. *Geomorphology* 92, 60–75.
- Bowman, D., Savoray, T., Devora, S., Shapira, I., Laronne, J.B., 2010. Extreme rates of channel incision and shape evolution in response to continuous, rapid base-level fall, the Dead Sea, Israel. *Geomorphology* 114, 227–237.
- Bowman, D., Devora, S., Svoray, T., 2011. Drainage organization on the newly emerged Dead Sea bed, Israel. *Quat. Int.* 233, 53–60.
- Bruins, H.J., Lithwick, H., 1998. *The Arid Frontier: Interactive Management of Environment and Development*. Kluwer, Dordrecht.
- Campbell, I.A., 1989. Badlands and badland gullies. In: Thomas, D.S.G. (Ed.), *Arid Zone Geomorphology*. Belhaven Press, London, pp. 159–183.
- Filin, S., Baruch, A., Avni, Y., Marco, S., 2011. Sinkhole characterization in the Dead Sea area using airborne laser scanning. *Nat. Hazards* 58, 1135–1154.
- Garfunkel, Z., Zak, I., Freund, R., 1981. Active faulting in the Dead Sea rift. *Tectonophysics* 80, 1–26.
- Glazovsky, N.F., 1995. The Aral Sea basin. Regions at risk: comparison of threatened environments. In: Kaspersion, J.X., Kaspersion, R.E., Turner II, B.L. (Eds.), *The Aral Sea Basin Regions at Risk: Comparison of Threatened Environments*. United Nations University Press, Tokyo, pp. 92–139.
- Hassan, M.A., Klein, M., 2002. Fluvial adjustment of the Lower Jordan River to a drop in the Dead Sea level. *Geomorphology* 4, 21–33.
- Horton, R.E., 1945. Erosional development of stream and their drainage basins: hydrophysical approach to quantitative morphology. *Bull. Geol. Soc. Am.* 59, 275–370.
- Ken-Tor, R., Agnon, A., Enzel, Y., Marco, S., Negendank, J.F.W., Stein, M., 2001. High-resolution geological record of historic earthquakes in the Dead Sea basin. *J. Geophys. Res.* 106, 2221–2234.
- Klein, C., Flohn, H., 1987. Contributions to the knowledge of the fluctuations of the Dead-Sea level. *Theor. Appl. Climatol.* 38, 151–156.
- Koss, J.E., Ethridge, F.G., Schumm, S.A., 1994. An experimental study of the effects of base level change on fluvial, coastal and shelf systems. *J. Sediment. Petrol.* B64, 90–98.
- Mainguet, M., 1991. *Desertification: Natural Background and Human Mismanagement*. Springer Series in Physical Environments, vol. 9. Springer Verlag, Heidelberg.

- Mainguet, M., Le'tolle, R., 1998. Human-made desertification in the Aral Sea Basin: planning and management failures. In: Bruins, H.J., Lithwick, H. (Eds.), *The Arid Frontier: Interactive Management of Environment and Development*. Kluwer Academic Publishers, Dordrecht, pp. 129–142.
- Mayer, L., 1990. *Introduction to Quantitative Geomorphology*. Prentice-Hall, Upper Saddle River (380 pp.).
- Schumm, S.A., 1993. River response to base level change: implications for sequence stratigraphy. *J. Geol.* 101, 279–294.
- Sneh, A., Bartov, Y., Rosensaft, M., 1998. Geological map of Israel, 1:200,000, Geological Survey of Israel, Jerusalem.
- Summerfield, M.A., 1991. *Global Geomorphology*. Longman, Essex.
- UNCCD, 1995. *United Nations Convention to Combat Desertification in Those Countries Experiencing Serious Drought and/or Desertification, Particularly in Africa*.
- UNYDD, 2006. *The United Nations General Assembly International Year of Deserts and Desertification*.
- Yecheili, Y., Magariz, M., Levy, Y., Weber, U., Kafri, U., Woelfli, W., Bonani, G., 1993. Late Quaternary geological history of the Dead Sea area, Israel. *Quat. Res.* 39, 59–67.
- Yecheili, Y., Abelson, M., Bein, A., Crouvi, O., Shtivelman, V., 2006. Sinkhole “swarms” along the Dead Sea coast: Reflection of disturbance of lake and adjacent groundwater systems. *Geol. Soc. Am. Bull.* 118, 1075–1087.